

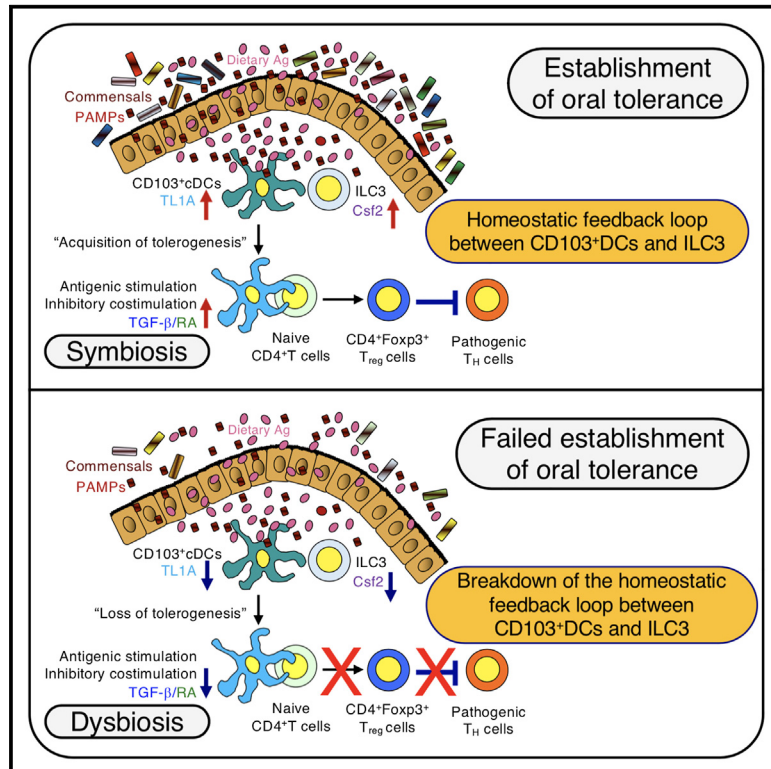


Gut dysbiosis promotes the breakdown of oral tolerance mediated through dysfunction of mucosal dendritic cells

メタデータ	言語: English 出版者: 公開日: 2023-04-26 キーワード (Ja): キーワード (En): dendritic cell, tolerogenesis, oral tolerance, mesenteric lymph nodes, dysbiosis, innate lymphoid cells, colony-stimulating factor 2, TNF-like ligand 1A 作成者: チョウジヨウフ, ナランツオツク, 菱川, 善隆, 佐藤, 克明, Fukaya, Tomohiro, Uto, Tomofumi, Mitoma, Shuya, Takagi, Hideaki, Nishikawa, Yotaro, Tominaga, Moe メールアドレス: 所属:
URL	http://hdl.handle.net/10458/00010600

Gut dysbiosis promotes the breakdown of oral tolerance mediated through dysfunction of mucosal dendritic cells

Graphical abstract



Authors

Tomohiro Fukaya, Tomofumi Uto, Shuya Mitoma, ..., Narantsog Choijookhuu, Yoshitaka Hishikawa, Katsuaki Sato

Correspondence

katsuaki_sato@med.miyazaki-u.ac.jp

In brief

Intestinal dysbiosis hampers the establishment of oral tolerance. Fukaya et al. provide insight into the underlying mechanisms by showing that intestinal dysbiosis impairs the crosstalk between CD103⁺ cDCs and ILC3s, which impairs the tolerogenesis of CD103⁺ cDCs, abolishing the establishment of oral tolerance.

Highlights

- CD103⁺ cDCs are prerequisite for establishing oral tolerance
- Intestinal dysbiosis leads to the abortive establishment of oral tolerance
- Intestinal dysbiosis results in loss of the tolerogenesis of CD103⁺ cDCs
- Intestinal dysbiosis hampers crosstalk between CD103⁺ cDCs and ILC3s



Article

Gut dysbiosis promotes the breakdown of oral tolerance mediated through dysfunction of mucosal dendritic cells

Tomohiro Fukaya,^{1,5} Tomofumi Uto,^{1,5} Shuya Mitoma,^{1,5} Hideaki Takagi,^{1,5} Yotaro Nishikawa,^{1,2} Moe Tominaga,^{1,3} Narantsog Choijookhuu,⁴ Yoshitaka Hishikawa,⁴ and Katsuaki Sato^{1,5,6,7,*}

¹Division of Immunology, Department of Infectious Diseases, Faculty of Medicine, University of Miyazaki, 5200 Kihara, Kiyotake, Miyazaki 889-1692, Japan

²Department of Dermatology, Faculty of Medicine, University of Miyazaki, 5200 Kihara, Kiyotake, Miyazaki 889-1692, Japan

³Department of Oral and Maxillofacial Surgery, Faculty of Medicine, University of Miyazaki, 5200 Kihara, Kiyotake, Miyazaki 889-1692, Japan

⁴Division of Histochemistry and Cell Biology, Department of Anatomy, Faculty of Medicine, University of Miyazaki, Miyazaki 889-1692, Japan

⁵Japan Agency for Medical Research and Development (AMED), 1-7-1 Otemachi, Chiyoda-ku, Tokyo 100-0004, Japan

⁶Frontier Science Research Center, University of Miyazaki, 5200 Kihara, Kiyotake, Miyazaki 889-1692, Japan

⁷Lead contact

*Correspondence: katsuaki_sato@med.miyazaki-u.ac.jp

<https://doi.org/10.1016/j.celrep.2023.112431>

SUMMARY

While dysbiosis in the gut is implicated in the impaired induction of oral tolerance generated in mesenteric lymph nodes (MesLNs), how dysbiosis affects this process remains unclear. Here, we describe that antibiotic-driven gut dysbiosis causes the dysfunction of CD11c⁺CD103⁺ conventional dendritic cells (cDCs) in MesLNs, preventing the establishment of oral tolerance. Deficiency of CD11c⁺CD103⁺ cDCs abrogates the generation of regulatory T cells in MesLNs to establish oral tolerance. Antibiotic treatment triggers the intestinal dysbiosis linked to the impaired generation of colony-stimulating factor 2 (Csf2)-producing group 3 innate lymphoid cells (ILC3s) for regulating the tolerogenesis of CD11c⁺CD103⁺ cDCs and the reduced expression of tumor necrosis factor (TNF)-like ligand 1A (TL1A) on CD11c⁺CD103⁺ cDCs for generating Csf2-producing ILC3s. Thus, antibiotic-driven intestinal dysbiosis leads to the breakdown of crosstalk between CD11c⁺CD103⁺ cDCs and ILC3s for maintaining the tolerogenesis of CD11c⁺CD103⁺ cDCs in MesLNs, responsible for the failed establishment of oral tolerance.

INTRODUCTION

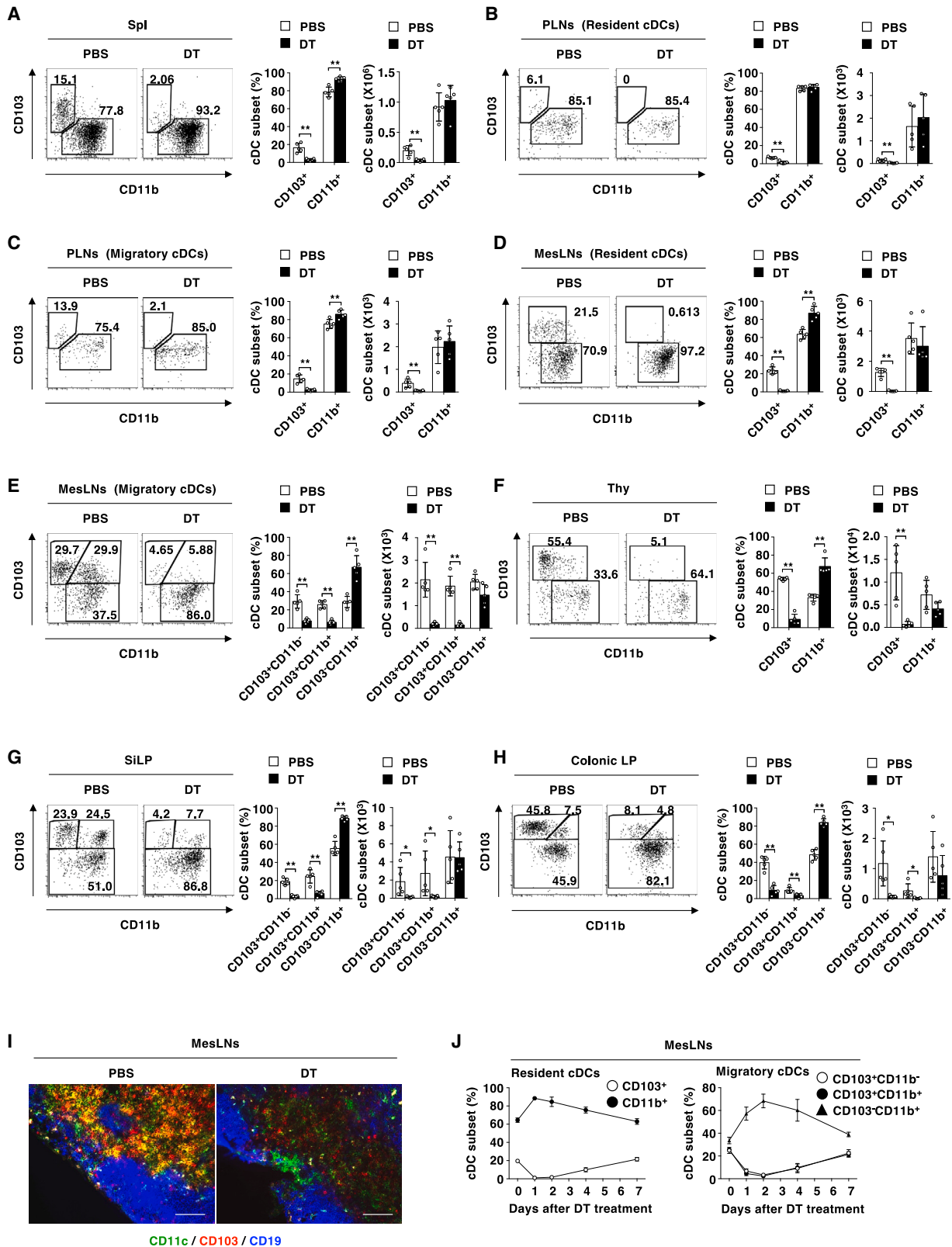
Dendritic cells (DCs) are essential antigen (Ag)-presenting cells (APCs) linking innate and adaptive immunity.^{1–3} DCs comprise heterogeneous subsets, functionally classified into conventional DCs (cDCs) and plasmacytoid DCs (pDCs).^{1–3} For the initiation of primary T cell responses against microbial infection, DCs recognize and process microbial Ag to present their antigenic peptides in the context of the major histocompatibility complex (MHC) in conjunction with costimulatory molecules and cytokines for the differentiation of naive T cells to effector T (T_{eff}) cells.^{1–3} Conversely, DCs are reportedly critical for the maintenance of immune homeostasis under steady-state and certain environmental conditions by generating immune tolerance through mechanisms involving CD4⁺Foxp3⁺ regulatory T (T_{reg}) cells that include self-reactive thymic-derived naturally occurring T_{reg} (tT_{reg}) cells and Ag-specific peripherally induced T_{reg} (pT_{reg}) cells generated from naive CD4⁺ T cells.³

In the gastrointestinal tract, the mucosal immune system distinguishes between harmful pathogenic microbes to initiate protective immune responses and harmless dietary constituents

and symbiotic microbes to induce unresponsiveness, known as oral tolerance to maintain intestinal immune homeostasis.⁴ Breakdown of this immune equilibrium leads to immunopathologies such as inflammatory bowel diseases (IBDs), food allergies, and invasive gastrointestinal infections.⁵ CD11c⁺CD103⁺ cDCs are considered to migrate to mesenteric lymph nodes (MesLNs) after sampling luminal Ags in the small intestine (SI), where there are privileged sites to establish oral tolerance.^{6,7} These mucosal CD11c⁺CD103⁺ cDCs imprint the tolerogenic properties, including the production of large quantities of retinoic acid (RA) and transforming growth factor (TGF)- β as well as prominent expressions of B7 family members of coinhibitory molecules (B7-H1 and B7-DC) to promote the intestinal emergence of CD4⁺Foxp3⁺ pT_{reg} cells to enforce oral tolerance.^{6–14}

Dysbiosis is the perturbation of the normal microbiota composition that could disrupt the symbiotic relationship between the host and associated microbes, which is induced by host genetics, microbial infection, and inflammation as well as environmental factors such as antibiotics, diet, vaccination, and sanitation.¹⁵ Accumulating evidence indicates that gut microbiota dysbiosis is associated with susceptibility to certain





(legend on next page)

immune disorders.^{16–18} As the use of antibiotics during infancy perturbs intestinal bacterial populations linked with an increased prevalence of allergic diseases,^{19–22} early life can be a critical window for the impact of the alteration of gut microbiota on immune dysregulation, leading to the promotion of a later increase in the prevalence of allergic conditions.^{23,24} In line with the requirement of gut microbiota for the establishment of oral tolerance,^{25–28} antibiotic administration reportedly hampered the induction of oral tolerance.^{29–31} However, how antibiotic-derived gut dysbiosis operates to impair the induction of oral tolerance by acting on intestinal cDCs remains unclear.

In this study, we demonstrate the prerequisite role of CD11c⁺CD103⁺ cDCs in the establishment of oral tolerance using binary transgenic (Tg) mice, which allow the selective conditional ablation of this cDC subset *in vivo*. Furthermore, the antibiotic-driven intestinal dysbiosis leads to the dysregulated tolerogenic function of CD11c⁺CD103⁺ cDCs through the impaired crosstalk with RA-related orphan receptor γ t (ROR γ t)⁺ group 3 innate lymphoid cells (ILC3s) in MesLNs that are responsible for abolishing the establishment of oral tolerance.

RESULTS

Generation of mice allowing inducible ablation of CD11c⁺CD103⁺ cDCs

It has been shown that mice with mutations of several transcription factor genes and Tg mice with cell-type-specific promoter-driven expression of diphtheria toxin (DT) or the DT receptor (DTR) allowed for the constitutive or inducible ablation of cDC lineages with mutual expressions of target molecules and CD103.³² In order to probe for the potential role of CD11c⁺CD103⁺ cDCs in immune responses, we developed mutant mice allowing specific elimination of CD11c⁺CD103⁺ cDCs. To this end, we generated *Cd103/Itgae-loxP* signal-flanked transcriptional STOP cassette (LSL)-DTR bacterial artificial chromosome (BAC) Tg mice (CD103-LSL-DTR mice) that harbor DTR behind LSL in the *Cd103/Itgae* locus and then crossed this strain with CD11c-Cre BAC Tg mice³³ to produce CD11c-Cre:CD103-LSL-DTR double-Tg mice (Figure S1), referred to as CD11c:CD103-DTR mice. Unexpectedly, a single injection of DT at 0.5–1 μ g/mouse (about 25–50 ng/g body weight) resulted in the death of CD11c:CD103-DTR mice within 10 days, which was similarly observed in CD11c-DTR/EGFP mice³⁴ and CD205-DTR mice.³⁵ Therefore, we generated bone marrow (BM) chimeric mice by reconstitution with BM from CD11c:CD103-DTR mice into lethally irradiated recipient wild-type (WT) mice (CD11c:CD103-DTR \rightarrow WT chimeras) and used them for subsequent experiments. Flow cytometric analysis of

CD11c:CD103-DTR \rightarrow WT chimeras revealed that CD11c⁺CD103⁺ cDCs were depleted in MesLNs as well as other lymphoid tissues after DT injection (Figures 1A–1H). On the other hand, the treatment of CD11c:CD103-DTR \rightarrow WT chimeras with DT led to normal frequencies of other leukocytes, while this treatment decreased or enhanced the frequency of CD8⁺ T cells or neutrophils (Figures S2A–S2H). Histological analysis confirmed the lack of CD11c⁺CD103⁺ cDCs in MesLNs of CD11c:CD103-DTR \rightarrow WT chimeras (Figure 1I). Furthermore, their near-complete elimination persisted for 2 days after the injection of DT in spleen (Spl) and MesLNs in CD11c:CD103-DTR \rightarrow WT chimeras, after which their proportions were gradually restored by 7 days, while reciprocal changes in the frequencies of their CD11c⁺CD103[−] counterparts were observed (Figures 1J and S2I). We also observed that the treatment of CD11c:CD103-DTR \rightarrow WT chimeras with DT led to marked elevation of the serum concentration of the Fms-related tyrosine kinase 3 ligand (Flt3L), which is known as critical for the development of DC lineages,³ in CD11c:CD103-DTR \rightarrow WT chimeras, and its production gradually decreased thereafter to the normal level (Figure S2J).

Collectively, CD11c:CD103-DTR \rightarrow WT chimeras show the selective ablation of CD11c⁺CD103⁺ cDCs upon DT treatment (called “ Δ CD11c⁺CD103⁺ cDC mice” hereafter).

While oral administration of ovalbumin (OVA) protein induced Ag-specific division of the transferred OT-II⁺CD4⁺ T cells or OT-I⁺CD8⁺ T cells^{35–37} in MesLNs in CD11c⁺CD103⁺ cDC-sufficient control mice (untreated CD11c:CD103-DTR \rightarrow WT chimeras), these responses were markedly diminished in Δ CD11c⁺CD103⁺ cDC mice (Figures S2K and S2L).

Collectively, these results indicate that the absence of CD11c⁺CD103⁺ cDCs reduces the Ag-specific priming of T cells *in vivo*.

CD11c⁺CD103⁺ cDCs are required for the establishment of oral tolerance to abolish allergic pathogenesis

Oral administration of OVA protein before systemic immunization with OVA protein inhibited the production of OVA-specific immunoglobulin G₁ (IgG₁) and the development of delayed-type hypersensitivity (DTH), indicated as ear swelling, in response to intradermal (i.d.) sensitization with OVA protein in CD11c⁺CD103⁺ cDC-sufficient control mice (Figures 2A–2C). On the other hand, OVA protein-fed Δ CD11c⁺CD103⁺ cDC mice exhibited enhanced production of OVA-specific antibody (Ab) and progression of DTH relative to OVA protein-fed control mice (Figures 2A–2C). Similarly, OVA protein feeding before systemic immunization with OVA protein not only inhibited productions of OVA-specific IgG₁ and IgE but also reduced the

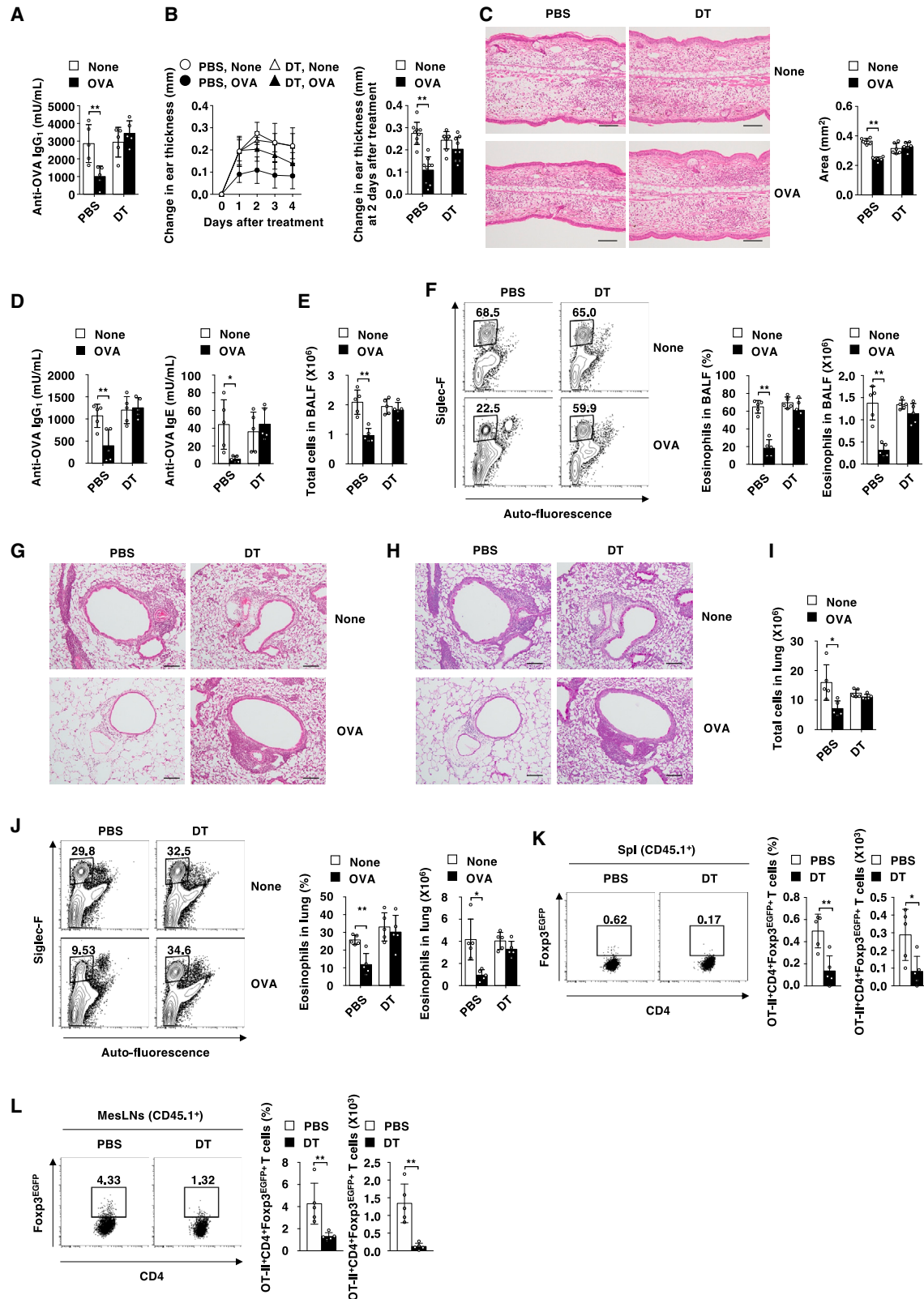
Figure 1. Inducible ablation of CD11c⁺CD103⁺ cDCs in Δ CD11c⁺CD103⁺ cDC mice

(A–H) Cell surface expression profile (left panel), proportion (middle panel), and absolute number (right panel) of cDC subset among I-A/I-E⁺CD11c⁺ cells in Spl (A); resident I-A/I-E⁺CD11c^{hi} cDCs in peripheral LNs (PLNs) (B); migratory I-A/I-E^{hi}CD11c⁺ cDCs in PLNs (C); resident I-A/I-E⁺CD11c^{hi} cDCs in MesLNs (D); migratory I-A/I-E^{hi}CD11c⁺ cDCs in MesLNs (E); I-A/I-E⁺CD11c⁺ cells in the thymus (Thy) (F); I-A/I-E⁺CD11c⁺ cells in small intestinal lamina propria (SiLP) (G); or I-A/I-E⁺CD11c⁺ cells in colonic LP (H).

(I) Representative frozen sections of MesLNs were stained for CD11c (green), CD103 (red), and CD19 (blue). Scale bars indicate 100 μ m.

(J) Frequency of cDC subset among resident I-A/I-E⁺CD11c^{hi} cDCs or migratory I-A/I-E^{hi}CD11c⁺ cDCs in MesLNs.

Data were obtained from three to five individual samples in a single experiment of at least three independent experiments. The data are shown from all pooled experiments. The p values are determined by unpaired two-tailed Student's t test. *p < 0.05, **p < 0.01.



(legend on next page)

manifestation of asthmatic symptoms in response to intranasal (i.n.) sensitization with OVA protein in CD11c⁺CD103⁺ cDC-sufficient control mice (Figures 2D–2J). In contrast, OVA protein feeding failed to suppress the production of OVA-specific Abs and the development of these asthmatic symptoms in Δ CD11c⁺CD103⁺ cDC mice (Figures 2D–2J).

While OVA protein feeding elicited the generation of Ag-specific OT-II⁺CD4⁺Foxp3^{EGFP+} pT_{reg} cells from transferred OT-II⁺CD4⁺Foxp3^{EGFP-} T cells^{14,35,36} in Spl and MesLNs in CD11c⁺CD103⁺ cDC-sufficient control mice, their generation was markedly impaired in Δ CD11c⁺CD103⁺ cDC mice (Figures 2K and 2L).

Taken together, these results indicate that the absence of CD11c⁺CD103⁺ cDCs inhibits the establishment of oral tolerance and *de novo* generation of Ag-specific CD4⁺Foxp3⁺ pT_{reg} cells in MesLNs upon oral antigenic application.

Antibiotic-driven infant gut dysbiosis abrogates the protective effect of oral tolerance against allergic pathogenesis

Oral combined antibiotic administration resulted in quantitative and qualitative alterations to commensal bacteria, but not fungi, colonizing SI, including reductions in bacteria of Proteobacteria, Bacteroidetes, and Actinobacteria when compared with control mice (Figure S3). Furthermore, oral combinatorial antibiotic treatment before exposure to Ag reduced the induction of oral tolerance to suppress the progression of the pathogenesis of DTH and allergic asthma (Figures 3A–3J).

Collectively, these results indicate that the antibiotic treatment prior to exposure to fed Ag prevents the induction of oral tolerance, which is associated with reductions of Proteobacteria, Bacteroidetes, and Actinobacteria in SI.

While Ag-specific generation of CD4⁺Foxp3⁺ pT_{reg} cells was reportedly reduced under germ-free (GF) conditions,³⁸ how oral combinatorial antibiotic treatment affects their *de novo* generation in the process of oral tolerance is less defined. Similar to the published report with the unchanged existence of aboriginal CD4⁺Foxp3⁺ T_{reg} cells in MesLNs under GF conditions,³⁹ oral combinatorial antibiotic treatment did not alter the frequency of aboriginal CD4⁺Foxp3⁺ T_{reg} cells in MesLNs (Figure S4A). On the other hand, oral combined antibiotic exposure inhibited Ag-specific generation of OT-II⁺CD4⁺Foxp3^{EGFP+} pT_{reg} cells in MesLNs upon oral antigenic priming (Figure 3K).

Collectively, these results indicate that antibiotic treatment prior to exposure to dietary Ag suppresses the generation of Ag-specific CD4⁺Foxp3⁺ pT_{reg} cells in MesLNs.

Antibiotic-driven gut dysbiosis causes the dysregulation of CD11c⁺CD103⁺ cDCs in MesLNs

Whereas the influence of GF conditions on the proportion of MesLN cDC subsets has been controversially reported,^{40,41} oral combinatorial antibiotic treatment had marked no effect on the ratio between resident MHC class II (I-A/I-E)⁺CD11c^{hi} cDCs and migratory I-A/I-E^{hi}CD11c⁺ cDCs among leukocytes in MesLNs in normal mice, although their absolute cell numbers were decreased (Figure 4A). On the other hand, oral exposure to combinatorial antibiotics reduced or enhanced the proportion of CD103⁺CD11b⁻ cDCs or CD103⁻CD11b⁺ cDCs in resident I-A/I-E⁺CD11c^{hi} cDCs (Figure 4B). Similarly, the proportion of CD103⁺CD11b⁻ cDCs was decreased upon oral combinatorial antibiotic exposure, whereas the proportions of CD103⁺CD11b⁺ cDCs and CD103⁻CD11b⁺ cDCs were increased in migratory I-A/I-E^{hi}CD11c⁺ cDCs (Figure 4C). Furthermore, oral combinatorial antibiotic treatment enhanced the cell surface expressions of CD80 and CD86 on migratory CD103⁺CD11b⁺ cDCs, whereas this treatment reduced the cell surface expressions of B7-H1 and B7-DC on migratory cDC subsets (Figure S4B).

Collectively, these results indicate that the antibiotic treatment affects the constituency of cDC subsets and their phenotypes in MesLNs.

CD103⁺ cDCs obtained from normal mice exhibited a superior ability to induce the Ag-specific generation of OT-II⁺CD4⁺Foxp3^{EGFP+} pT_{reg} cells from OT-II⁺CD4⁺Foxp3^{EGFP-} T cells than CD103⁻ cDCs in MesLNs in the presence or absence of the active or latent form of TGF- β , whereas oral combinatorial antibiotic exposure reduced their generation in the presence or absence of the latent form of TGF- β (Figures 4D–4F).

Both resident cDC subsets exhibited a higher transcriptional expression of *Tgfb1* than migratory cDC subsets, whereas migratory CD103⁺CD11b⁻ cDCs displayed a higher transcriptional expression of *Itgb8* for the activation of TGF- β ^{8,13,14} than their counterparts (Figure 4G). On the other hand, migratory CD103⁺CD11b⁻ cDCs showed a higher expression of *Aldh1a2* encoding RA-generating enzyme retinal dehydrogenase 2 (RALDH2)^{4,14} and activity of aldehyde dehydrogenase (ALDH)

Figure 2. Ablation of CD11c⁺CD103⁺ cDCs abrogates the establishment of oral tolerance

- (A) Serum level of OVA-specific IgG₁.
 (B) OVA-specific DTH indicated as ear thickness.
 (C) Representative hematoxylin and eosin (H&E) sections (magnification 200 \times) of ear skin (left panel), and the area of the epidermis and dermis of ear sections (right panel). Scale bars indicate 100 μ m.
 (D) Serum levels of OVA-specific IgG₁ (left panel) and OVA-specific IgE (right panel).
 (E) Absolute cell numbers of total bronchoalveolar lavage fluid (BALF) cells.
 (F) Cell surface expression profile (left panel), proportion (middle panel), and absolute number (right panel) of eosinophils in BALF.
 (G and H) H&E (G) and periodic acid-Schiff (PAS; H) sections (magnification 200 \times) of lung tissues. Scale bars indicate 100 μ m.
 (I) Absolute cell numbers of total leukocytes in lung tissues.
 (J) Cell surface expression profile (left panel), proportion (middle panel), and absolute number (right panel) of eosinophils in lung tissues.
 (K and L) Cell surface expression profile (left panel), proportion (middle panel), and absolute number (right panel) of CD45.1⁺OT-II CD4⁺Foxp3^{EGFP+} T cells in Spl (K) and MesLNs (L).

Data were obtained from three to ten individual samples in a single experiment of at least three independent experiments. The data are shown from all pooled experiments. The p values are determined by unpaired two-tailed Student's t test. *p < 0.05, **p < 0.01.

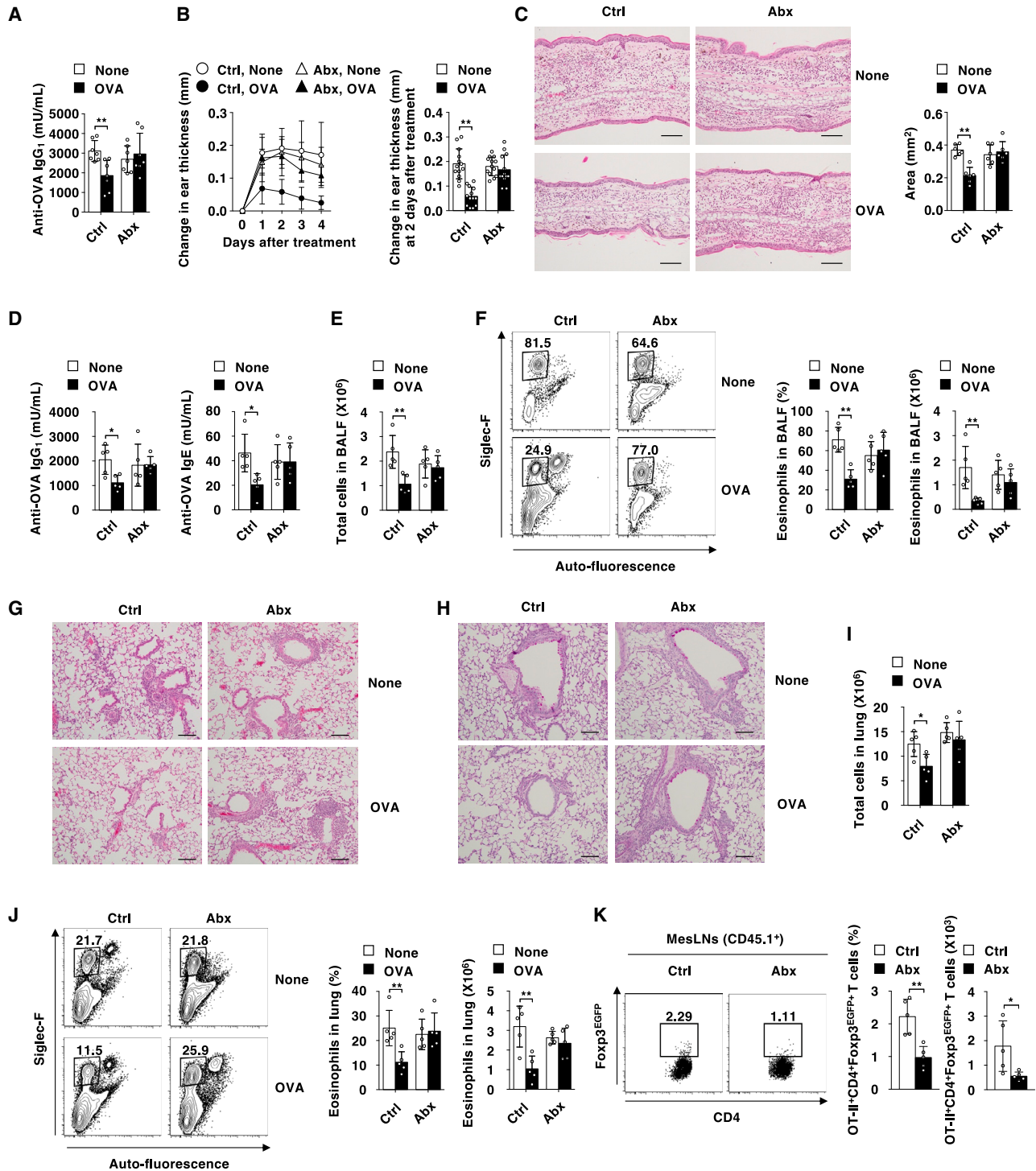


Figure 3. Antibiotic-driven gut dysbiosis abrogates the establishment of oral tolerance

(A) Serum level of OVA-specific IgG₁.
 (B) OVA-specific DTH indicated as ear thickness.
 (C) Representative H&E sections (magnification 200×) of ear skin (left panel) and the area of the epidermis and dermis of ear sections (right panel). Scale bars indicate 100 μm.
 (D) Serum level of OVA-specific IgG₁ (left panel) and OVA-specific IgE (right panel).
 (E) Absolute cell numbers of total BALF cells.
 (F) Cell surface expression profile (left panel), proportion (middle panel), and absolute number (right panel) of eosinophils in BALF.
 (legend continued on next page)

than other migratory cDC subsets as well as resident cDC subsets (Figures 4G–4I). However, oral combinatorial antibiotic treatment reduced the transcriptional expression of *Itgb8* in migratory CD103⁺CD11b[−] cDCs and CD103[−]CD11b⁺ cDCs (Figure 4G). Furthermore, oral combinatorial antibiotic treatment not only reduced the transcriptional expression of *Aldh1a2* in migratory CD103⁺CD11b[−] cDCs but also inhibited the activity of ALDH in resident cDC subsets, migratory CD103⁺CD11b[−] cDCs, and migratory CD103[−]CD11b⁺ cDCs (Figures 4G–4I).

Taken together, these results indicate that the antibiotic treatment regulates the capacity of MesLN CD11c⁺ cDC subsets to generate CD4⁺Foxp3⁺ pT_{reg} cells.

Antibiotic-driven gut dysbiosis reduces the expressions of Csf2 on RORγt⁺ ILC3s and TL1A on CD11c⁺CD103⁺ cDCs in MesLNs

It has been shown that colony-stimulating factor 2 (Csf2), also known as granulocyte-macrophage CSF (GM-CSF), is critical for the homeostasis and function of colonic cDCs and macrophages, and RORγt⁺ ILC3s are a primary source of Csf2 in the noninflamed gut.⁴² Similar to the published report,⁴³ RORγt⁺ ILC3s were found in the interfollicular area where CD11c⁺ cDCs and CD4⁺Foxp3⁺ T_{reg} cells localized in MesLNs in WT mice (Figure S5). RORγt⁺ ILC3s displayed a higher expression of Csf2 than other immune cells in MesLNs in WT mice, whereas oral combinatorial antibiotic exposure mainly suppressed the expression of Csf2 on RORγt⁺ ILC3s (Figures 5A and S6A).

Collectively, these results indicate that the antibiotic treatment reduces the expression of Csf2 on RORγt⁺ ILC3s in MesLNs.

Whereas RORγt⁺ ILC3-driven Csf2 production has been shown to be dependent on the ability of intestinal macrophages to sense microbiota and produce interleukin (IL)-1β in the gut,⁴² oral combinatorial antibiotic exposure had little or no effect on expression of the *Il1b* transcript in CD11c⁺ cDCs or leukocytes in MesLNs (Figures 5B and S6B).

Microbiota-induced production of tumor necrosis factor (TNF)-like ligand 1 A (TL1A) release from CX3CR1⁺ mononuclear phagocytes (MNP) has been shown to drive RORγt⁺ ILC3s to produce IL-22 for protection against acute colitis.⁴⁴ On the other hand, the activation of signaling through death receptor (DR)3, known as a receptor for TL1A, by an agonistic anti-DR3 monoclonal Ab (mAb) reportedly increased the production of Csf2 from RORγt⁺ ILC3s.⁴⁵ In line with reduced expression of the *Tnfrsf15* transcript for TL1A in CD11c⁺ cDCs as well as leukocytes in MesLNs of antibiotic-treated mice (Figures 5B and S6B), oral combinatorial antibiotic exposure suppressed the expression of TL1A on resident and migratory cDC subsets as well as macrophages and B cells in MesLNs (Figures 5C and S6C). Indeed, both resident and migratory CD103⁺CX3CR1⁺ cDC and CD103[−]CX3CR1[−] cDC subsets exhibited reduced

expression of TL1A upon oral combinatorial antibiotic exposure (Figures 5D, 5E, and S6D).

Taken together, these results indicate that the antibiotic treatment reduces the expression of TL1A on CD11c⁺CD103⁺ cDCs as well as other leukocytes in MesLNs.

CD11c⁺CD103⁺ cDCs are required for the generation of Csf2⁺RORγt⁺ ILC3s and expression of TL1A in MesLNs

ΔCD11c⁺CD103⁺ cDC mice exhibited reductions in transcriptional expressions of *Tnfrsf15* and *Csf2*, but not *Il1b*, in leukocytes as well as the proportion of Csf2-producing RORγt⁺ ILC3s in MesLNs compared with CD11c⁺CD103⁺ cDC-sufficient control mice (Figures S6E and S6F).

Therefore, these results indicate that the absence of CD11c⁺CD103⁺ cDCs reduces expressions of TL1A and Csf2 as well as the generation of Csf2-producing RORγt⁺ ILC3s in MesLNs.

For the generation of mutant mice harboring CD11c⁺CD103⁺*Tl1a*^{−/−} cDCs, CD11c:CD103-DTR/*Tl1a*^{−/−} → WT mixed chimeras, which were generated by reconstitution with BM from CD11c:CD103-DTR mice and *Tl1a*^{−/−} mice (Figures S7A–S7E) into lethally irradiated recipient WT mice, received DT injection. As expected, CD11c⁺CD103⁺ cDCs in MesLNs were deficient for the expression of TL1A in CD11c:CD103-DTR/*Tl1a*^{−/−} → WT mixed chimeras after DT injection (called “CD11c⁺CD103⁺*Tl1a*^{−/−} cDC mice” hereafter), whereas they showed its expression in CD11c:CD103-DTR/WT → WT mixed chimeras (called “control mice” hereafter) (Figure S7F). OVA protein-fed CD11c⁺CD103⁺*Tl1a*^{−/−} cDC mice exhibited greater production of OVA-specific Abs and responses of DTH after systemic immunization with OVA protein than OVA protein-fed control mice (Figures S7G and S7H). Furthermore, OVA protein-fed CD11c⁺CD103⁺*Tl1a*^{−/−} cDC mice showed lower-level generation of Ag-specific OT-II⁺CD4⁺Foxp3^{EGFP+} pT_{reg} cells from transferred OT-II⁺CD4⁺Foxp3^{EGFP−} T cells in MesLNs than OVA protein-fed control mice (Figure S7I), while they had a similar frequency of aboriginal CD4⁺Foxp3⁺ T_{reg} cells in MesLNs (Figure S7J). On the other hand, CD11c⁺CD103⁺*Tl1a*^{−/−} cDC mice displayed a lower proportion of Csf2-producing RORγt⁺ ILC3 in MesLNs than control mice (Figure S7K).

Therefore, these results indicate that the deficiency of TL1A in CD11c⁺CD103⁺ cDCs not only impairs the establishment of oral tolerance and *de novo* generation of Ag-specific CD4⁺Foxp3⁺ pT_{reg} cells in MesLNs following oral antigenic application but also the induction of Csf2-producing RORγt⁺ ILC3 in MesLNs.

Csf2 improves gut dysbiosis-driven dysregulated tolerogenic function of MesLN CD11c⁺CD103⁺ cDCs

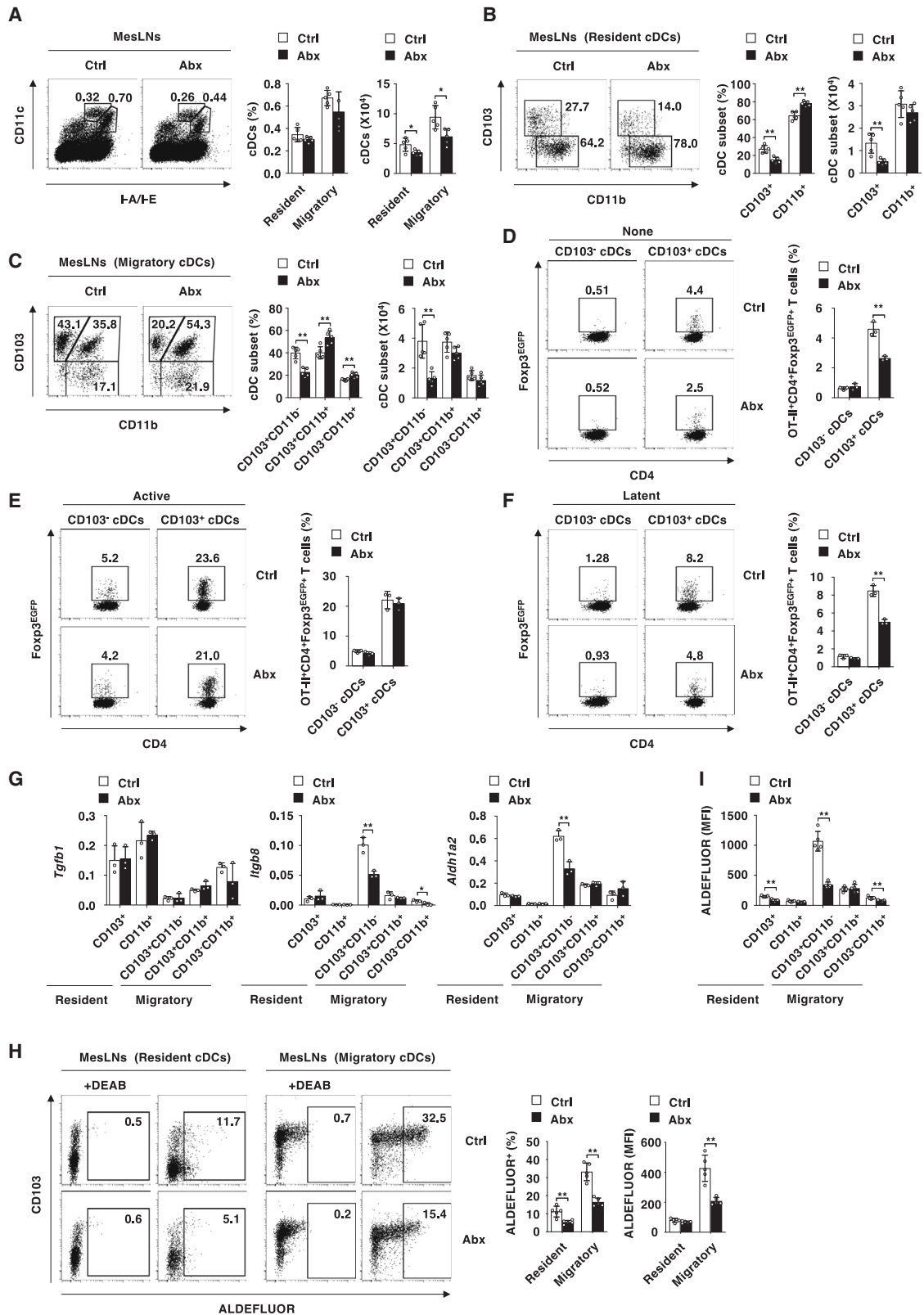
Stimulation with Csf2 enhanced the activity of ALDH as well as expressions of B7-DC, but not B7-H1, in MesLN CD11c⁺ cDCs obtained from antibiotic-treated dysbiotic mice (Figure S6G).

(G and H) H&E (G) and PAS (H) sections (magnification 200×) of lung tissues. Scale bars indicate 100 μm.

(I) Absolute cell numbers of total leukocytes in lung tissues.

(J) Cell surface expression profile (left panel), proportion (middle panel), and absolute number (right panel) of eosinophils in lung tissues.

(K) Cell surface expression profile (left panel), proportion (middle panel), and absolute number (right panel) of CD45.1⁺OT-II CD4⁺Foxp3^{EGFP+} T cells in MesLNs. Data were obtained from three to thirteen individual samples in a single experiment of at least three independent experiments. The data are shown from all pooled experiments. The p values are determined by unpaired two-tailed Student's t test. *p < 0.05, **p < 0.01.



(legend on next page)

Given the improvement of the dysfunction of MesLN CD11c⁺ cDCs obtained from the antibiotic-driven dysbiotic mice by supplementation of Csf2, and to gain further insight into how Csf2 may act on MesLN CD11c⁺ cDC subsets *in vivo*, we compared their constituency in normal mice and antibiotic-treated mice transplanted with B16-F10 melanoma cells (B16) or B16 that overexpressed Csf2 (B16^{Csf2}).⁴⁶ Transplantation with B16^{Csf2} enhanced the proportion and absolute cell numbers of migratory I-A/I-E^{hi}CD11c⁺ cDCs, but not resident I-A/I-E⁺CD11c^{hi} cDCs, among leukocytes in MesLNs of normal mice and the antibiotic-treated mice when compared with those transplanted with B16 (Figures S8A and S8B). In MesLNs, transplantation with B16^{Csf2} enhanced the proportion and absolute cell numbers of CD103⁺CD11b⁻ cDCs in resident I-A/I-E⁺CD11c^{hi} cDCs, whereas it enhanced the absolute cell numbers of CD103⁺CD11b⁻ cDCs and CD103⁺CD11b⁺ cDCs in migratory I-A/I-E^{hi}CD11c⁺ cDCs (Figures S8A and S8B).

Transplantation with B16^{Csf2} enhanced the expression level of B7-DCs, but not B7-H1, on CD103⁺CD11b⁻ cDCs and CD103⁺CD11b⁺ cDCs in migratory I-A/I-E^{hi}CD11c⁺ cDCs in MesLNs of normal mice and the antibiotic-treated mice when compared with those transplanted with B16 (Figure S8C). On the other hand, transplantation with B16^{Csf2} enhanced the ALDH activity in the subsets of resident I-A/I-E⁺CD11c^{hi} cDCs and migratory I-A/I-E^{hi}CD11c⁺ cDCs in MesLNs of normal mice and the antibiotic-treated mice when compared with those transplanted with B16 (Figures 5F–5I).

Transplantation with B16^{Csf2} enhanced Ag-specific generation of OT-II⁺CD4⁺Foxp3^{EGFP+} pT_{reg} cells in MesLNs during oral combinatorial antibiotic treatment (Figure S8D), whereas it had little or no effect on the proportion of aboriginal CD4⁺Foxp3⁺ T_{reg} cells in MesLNs (Figure S8E). Furthermore, transplantation with B16^{Csf2} enhanced the ability of CD11c⁺CD103⁺ cDCs obtained from MesLNs of normal mice and antibiotic-treated mice to induce the Ag-specific generation of OT-II⁺CD4⁺Foxp3^{EGFP+} pT_{reg} cells in the presence of the active or latent form of TGF-β (Figures S8F–S8H).

Therefore, these results indicate that Csf2 restores the gut dysbiosis-driven dysregulated tolerogenic function of MesLN CD11c⁺CD103⁺ cDCs.

RORγt⁺ ILC3-derived Csf2 upon activation of signaling through DR3 improves the gut dysbiosis-driven dysregulated tolerogenic function of MesLN CD11c⁺CD103⁺ cDCs

While RORγt⁺ ILC3s exhibited a higher expression of DR3 than other leukocytes in MesLNs, oral combinatorial antibiotic expo-

sure primarily suppressed the expression of DR3 on RORγt⁺ ILC3s (Figure S9A). Indeed, the administration of agonistic anti-DR3 mAb mainly enhanced the expression of Csf2 on RORγt⁺ ILC3s in the antibiotic-driven dysbiotic mice as well as normal mice (Figures 6A and 6B). Furthermore, the administration of agonistic anti-DR3 mAb had a similar effect to transplantation with B16^{Csf2} for the proportional changes of MLN CD11c⁺ cDC subsets and their enhanced expressions of B7-H1 and B7-DC as well as the reinforced activity of ALDH (Figures 6C–6F and S9B–S9D). We also observed that the treatment of normal mice or the antibiotic-treated mice with agonistic anti-DR3 mAb strengthened the ability of CD11c⁺CD103⁺ cDCs in MesLNs to induce the Ag-specific generation of OT-II⁺CD4⁺Foxp3^{EGFP+} pT_{reg} cells in the presence of the active or latent form of TGF-β (Figures 6G–6I).

Taken together, these results indicate that RORγt⁺ ILC3-derived Csf2 upon activation of signaling through DR3 restores the gut dysbiosis-driven dysregulated tolerogenic function of MesLN CD11c⁺CD103⁺ cDCs.

Agonistic anti-DR3 mAb improves the impaired protective effect of oral tolerance against allergic pathogenesis in antibiotic-driven dysbiotic mice

While the administration of agonistic anti-DR3 mAb had little or no effect on the induction of oral tolerance upon oral exposure of Ag to inhibit progression of the pathogenesis of DTH in normal mice, this treatment overcame the reduced induction of oral tolerance in the antibiotic-treated mice (Figures 7A–7D). Indeed, the administration of agonistic anti-DR3 mAb enhanced Ag-specific generation of OT-II⁺CD4⁺Foxp3^{EGFP+} pT_{reg} cells following oral antigenic priming as well as the proportion of aboriginal CD4⁺Foxp3⁺ T_{reg} cells in MesLNs in both normal and antibiotic-treated mice (Figures 7E and 7F).

While the administration of agonistic anti-DR3 mAb did not alter the induction of oral tolerance to inhibit the development of DTH in CD11c⁺CD103⁺ cDC-sufficient control mice following oral antigenic application, the administration of agonistic anti-DR3 mAb failed to enhance the induction of oral tolerance in ΔCD11c⁺CD103⁺ cDC mice (Figures 7G–7J). On the other hand, the administration of agonistic anti-DR3 mAb enhanced Ag-specific generation of OT-II⁺CD4⁺Foxp3^{EGFP+} pT_{reg} cells following oral antigenic priming in CD11c⁺CD103⁺ cDC-sufficient control mice, whereas their generation was markedly impaired in ΔCD11c⁺CD103⁺ cDC mice (Figure 7K). Similar to the published report in which treatment of mice with agonistic anti-DR3 mAb led to the expansion of CD4⁺Foxp3⁺ T_{reg} cells,⁴⁷ the administration of agonistic anti-DR3 mAb enhanced the

Figure 4. Antibiotic-driven gut dysbiosis impairs the capacity of MesLN cDC subsets to generate CD4⁺Foxp3⁺ pT_{reg} cells

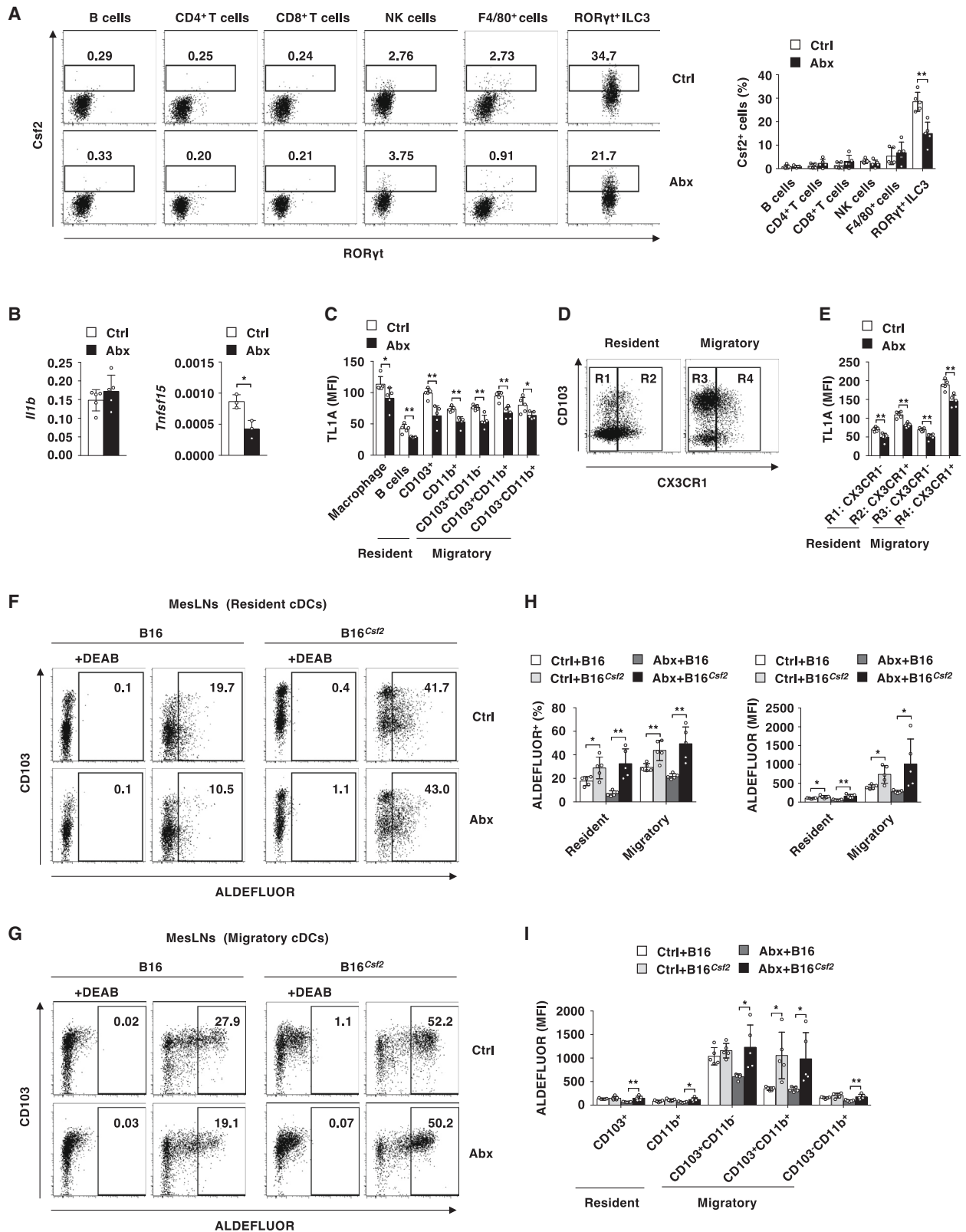
(A–C) Cell surface expression profile (left panel), proportion (middle panel), and absolute number (right panel) of CD11c⁺I-A/I-E⁺ cDCs among leukocytes (A); CD103⁺CD11b⁻ cDCs, CD103⁺CD11b⁺ cDCs, or CD103⁻CD11b⁺ cDCs among resident I-A/I-E⁺CD11c^{hi} cDCs (B); or migratory I-A/I-E^{hi}CD11c⁺ cDCs (C).

(D–F) Cell surface expression profile (left panel) and proportion (right panel) of CD45.1⁺OT-II⁺CD4⁺Foxp3^{EGFP+} T cells generated from CD45.1⁺OT-II⁺CD4⁺Foxp3^{EGFP+} T cells cultured with cDCs in the absence (D) or presence (E) or latent (F) form of TGF-β.

(G) Transcriptional expressions of *Tgfb1*, *Itgb8*, and *Aldh1a2* in cDC subset in MesLNs.

(H and I) Cell surface expression profile (H, left panel) and proportion (H, middle panel) of ALDEFUOR⁺ cells, and mean fluorescence intensity (MFI) of ALDEFUOR in cDC subset (H, right panel, and I) in MesLNs.

Data were obtained from three to five individual samples in a single experiment of at least three independent experiments. The data are shown from all pooled experiments. The p values are determined by unpaired two-tailed Student's t test. *p < 0.05, **p < 0.01.



(legend on next page)

proportion of aboriginal CD4⁺Foxp3⁺ T_{reg} cells in MesLNs in both CD11c⁺CD103⁺ cDC-sufficient control mice and ΔCD11c⁺CD103⁺ cDC mice (Figure 7L).

Therefore, these results indicate that agonistic anti-DR3 mAb restores the gut dysbiosis-driven impaired protective effect of oral tolerance against allergic pathogenesis and generation of Ag-specific CD4⁺Foxp3⁺ pT_{reg} cells in MesLNs required for CD11c⁺CD103⁺ cDCs.

In small intestinal lamina propria (SiLP), oral combinatorial antibiotic treatment reduced the activity of ALDH in CD103⁺CD11b⁻ cDCs but not other cDC subsets, whereas this treatment had little or no effect on the proportions of cDC subsets as well as their expression levels of B7-H1 and B7-DC (Figures S10A–S10J). On the other hand, transplantation with B16^{Csf2} or the administration of agonistic anti-DR3 mAb failed to enhance the activity of ALDH in cDC subsets in SiLP (Figures S10A, S10B, S10F, and S10G). Furthermore, the administration of agonistic anti-DR3 mAb, but not transplantation with B16^{Csf2}, only enhanced the proportion of CD103⁻CD11b⁺ cDCs, whereas both treatments enhanced the expression level of B7-DC on CD103⁻CD11b⁺ cDCs but not other cDC subsets in SiLP (Figures S10C–S10E and S10H–S10J).

Taken together, these results indicate that antibiotic treatment affects the tolerogenic feature of CD11c⁺ cDCs in MesLNs more than those in SiLP.

CD103⁺CD11b⁻ cDCs and CD103⁺CD11b⁺ cDCs in SiLP showed a higher expression of Csf2 receptor α-chain (Csf2Rα) than those in MesLNs, while CD103⁻CD11b⁺ cDCs in MesLNs and SiLPs had its similar expression level (Figure S11A). On the other hand, the expression level of Csf2Rβ on CD11c⁺ cDC subsets in SiLP was lower than those in MesLNs (Figure S11B).

Oral combinatorial antibiotic exposure suppressed the expression of Csf2 on RORγt⁺ ILC3s in SiLP (Figure S11C) as well as MesLNs (Figures 5A and 6A). On the other hand, CD103⁺CD11b⁺ cDCs in SiLP displayed a higher expression of TL1A than those in MesLNs, while similar expression levels of TL1A were observed in CD103⁺CD11b⁻ cDCs and CD103⁻CD11b⁺ cDCs in MesLNs and SiLP (Figures S6C and S11D). Different from the reduced expression of TL1A on migratory cDC subsets in MesLNs upon oral combinatorial antibiotic exposure (Figures 5C and S6C), this treatment reduced its expression on CD103⁺CD11b⁺ cDCs, but not CD103⁺CD11b⁻ cDCs or CD103⁻CD11b⁺ cDCs, in SiLP (Figure S11D).

Collectively, these results indicate that migratory cDC subsets exhibit different expressions of Csf2Rs and TL1A between

MesLNs and SiLP under normal and antibiotic-driven dysbiotic conditions.

DISCUSSION

In this study, our findings reveal that the antibiotic-driven intestinal dysbiosis hampers the crosstalk between CD11c⁺CD103⁺ cDCs and RORγt⁺ ILC3s in MesLNs that cause the dysfunctional regulation of the tolerogenesis of CD11c⁺CD103⁺ cDCs to abolish the establishment of oral tolerance.

Transient or constitutive loss of CD11c⁺ cDCs reportedly led to the enhanced proportion of granulocytes, possibly due to increased serum amounts of Flt3L.^{48–50} These phenomena led us to hypothesize that CD11c⁺CD103⁺ cDCs are responsible for the major consumption of Flt3L *in vivo*, while their absence leads to the release of excess amounts of Flt3L in the periphery, resulting in the expansion of neutrophils. Having demonstrated the reduction of the proportion of CD8⁺ T cells in lymphoid tissues with no change in the constituency of thymocytes in the absence of CD11c⁺CD103⁺ cDCs, CD11c⁺CD103⁺ cDCs could contribute to the peripheral expansion of CD8⁺ T cells. Given the impairment of Ag-specific priming of CD4⁺ T cells and CD8⁺ T cells in MesLNs upon oral antigenic application in the absence of CD11c⁺CD103⁺ cDCs, CD11c⁺CD103⁺ cDCs could be major APCs for the induction of Ag-specific T cell responses in MesLNs.

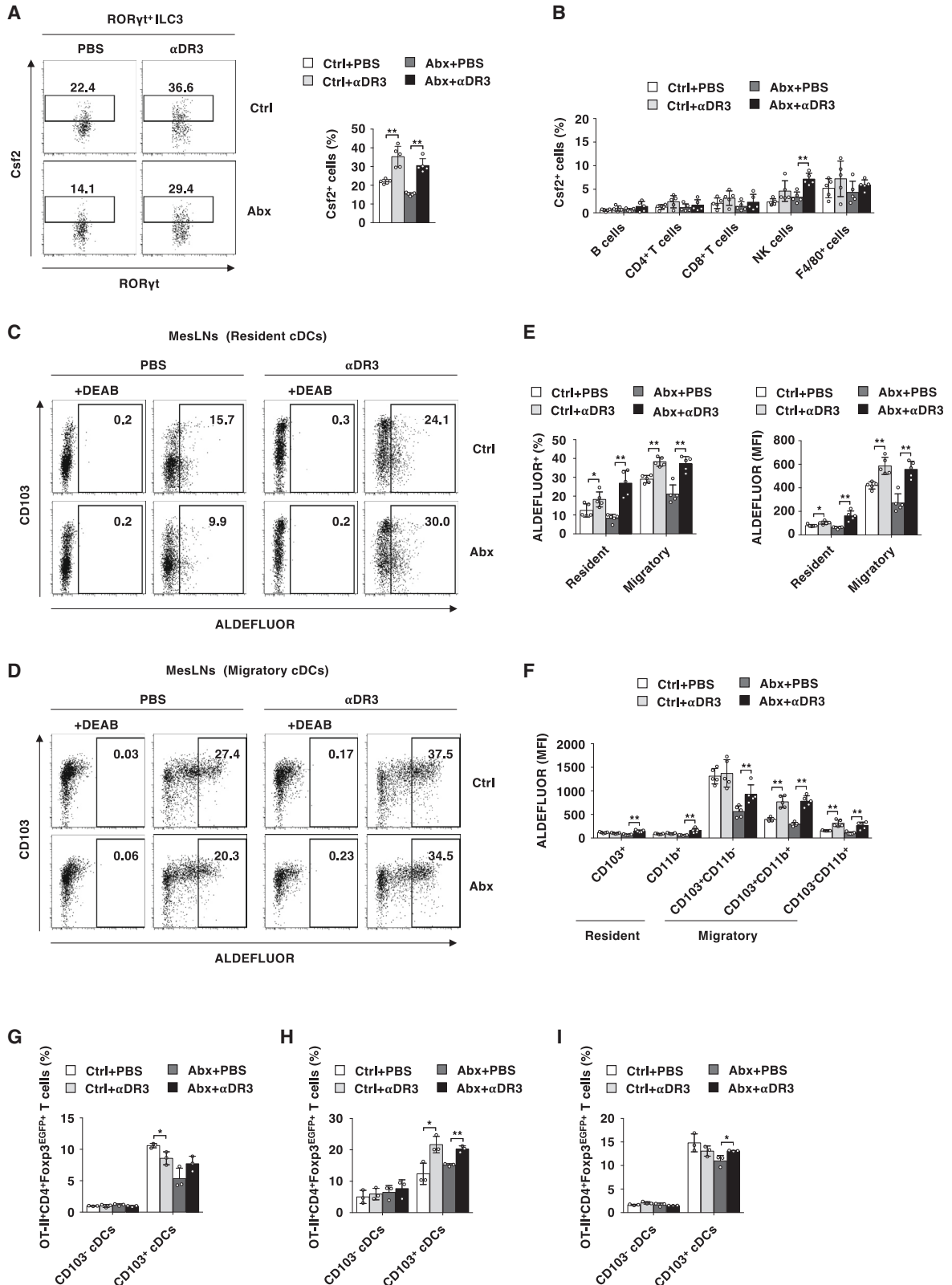
Batf3^{-/-} mice or zDC-Cre:*Irf8*^{fl/fl} mice lacking CD11c⁺CD103⁺CD11b⁻ cDC1s reportedly showed an almost normal induction of oral tolerance and partial inhibition of the generation of Ag-specific CD4⁺Foxp3⁺ T_{reg} cells.^{8,11} Furthermore, CD11c⁺CD103⁺CD11b⁺ cDC2s and CD11c⁺CD103⁻CD11b⁺cDC2s were reportedly inferior to CD11c⁺CD103⁺CD11b⁻ cDC1s in their capacity to generate Ag-specific CD4⁺Foxp3⁺ T_{reg} cells.^{6–8,13,14} Therefore, cDC1s or cDC2s alone could not generate an adequate number of Ag-specific CD4⁺Foxp3⁺ pT_{reg} cells to establish oral tolerance. On the other hand, the deficiency of CD11c⁺CD103⁺ cDCs caused the impaired establishment of oral tolerance and the reduced generation of Ag-specific CD4⁺Foxp3⁺ pT_{reg} cells in MesLNs upon oral antigenic application. Therefore, both CD11c⁺CD103⁺CD11b⁻ cDC1s and CD11c⁺CD103⁺CD11b⁺ cDC2s could be required for the sufficient generation of Ag-specific CD4⁺Foxp3⁺ pT_{reg} cells in MesLNs to establish oral tolerance.

Despite increasing epidemiological evidence that supports a link between exposure to antibiotics to alter normal infant gut microbiota and the enhancement of later susceptibility to allergic

Figure 5. Antibiotic-driven gut dysbiosis decreases expressions of Csf2 on RORγt⁺ ILC3s and TL1A on CD11c⁺CD103⁺ cDCs in MesLNs

- (A) Intracellular cytokine expression profile of Csf2-producing cells among RORγt⁺ ILC3s in MesLNs (left panel) and proportion of Csf2-producing cells among leukocytes in MesLNs (right panel).
 (B) Transcriptional expressions of *I11b* (left panel) and *Tnfrsf15* (right panel) in cDCs in MesLNs.
 (C) MFI of the expression of TL1A on leukocytes in MesLNs.
 (D) Cell surface expression profile of CD103 and CX3CR1 on resident I-A/I-E⁺CD11c^{hi} cDCs and migratory I-A/I-E^{hi}CD11c⁺ cDCs in MesLNs.
 (E) MFI of the expression of TL1A on subset of resident I-A/I-E⁺CD11c^{hi} cDCs and migratory I-A/I-E^{hi}CD11c⁺ cDCs in MesLNs.
 (F and G) Cell surface expression profile of ALDEFLUOR⁺ cells among resident I-A/I-E⁺CD11c^{hi} cDCs (F) and migratory I-A/I-E^{hi}CD11c⁺ cDCs (G) in MesLNs.
 (H) Proportion of ALDEFLUOR⁺ cells in resident I-A/I-E⁺CD11c^{hi} cDCs and migratory I-A/I-E^{hi}CD11c⁺ cDCs (left panel) and their MFI of ALDEFLUOR (right panel) in MesLNs.
 (I) MFI of ALDEFLUOR in cDCs subset in MesLNs.

Data were obtained from three to five individual samples in a single experiment of at least three independent experiments. The data are shown from all pooled experiments. The p values are determined by unpaired two-tailed Student's t test. *p < 0.05, **p < 0.01.



(legend on next page)

disorders,^{19–23} there is little known about how antibiotics-induced alteration of microbial composition during infancy affects the program for the establishment of oral tolerance.^{29–31} Analysis of antibiotic-treated mice suggests that the antibiotic-driven intestinal dysbiosis impaired the generation of Ag-specific CD4⁺Foxp3⁺pT_{reg} cells, leading to the impaired establishment of oral tolerance.

Although MesLN cDC subsets have been suggested to play a critical role in establishing oral tolerance,^{6–14} how antibiotic-driven gut dysbiosis affects their tolerogenic features is largely unclear. The oral combinatorial antibiotic treatment enhanced or reduced the expressions of the B7 family of costimulatory or coinhibitory molecules on migratory cDC subsets in MesLNs. Furthermore, this treatment impaired the ability of CD11c⁺CD103⁺ cDCs in MesLNs to induce Ag-specific CD4⁺Foxp3⁺pT_{reg} cells and generate the active form of TGF-β and RA. Therefore, our results suggest that the antibiotic-driven intestinal dysbiosis dysregulates the tolerogenic functions of CD11c⁺CD103⁺CD11b⁻ cDC1s and CD11c⁺CD103⁺CD11b⁺ cDC2s in MesLNs, which mediates the breakdown of oral tolerance.

It has been shown that Csf2 plays a critical role in the maintenance of cDC homeostasis and function, and RORγt⁺ ILC3 serves as its main source in intestinal tissues in response to stimulation with IL-1β or TL1A under homeostatic conditions.^{42,45} Furthermore, ILC3-derived IL-2 was reportedly essential for maintaining CD4⁺Foxp3⁺T_{reg} cells to establish immunological homeostasis and oral tolerance of dietary Ags in SI.⁵¹ Having demonstrated the localization of CD11c⁺ cDCs, RORγt⁺ ILC3s, and CD4⁺Foxp3⁺T_{reg} cells in the interfollicular area in MesLNs, the interfollicular area in MesLNs might provide a critical micro-environment for communication between CD11c⁺CD103⁺ cDCs and RORγt⁺ ILC3s to support the generation of Ag-specific CD4⁺Foxp3⁺pT_{reg} cells in establishing oral tolerance.

The absence of CD11c⁺CD103⁺ cDCs reduced the productions of TL1A and Csf2 as well as the emergence of Csf2-producing RORγt⁺ ILC3s in MesLNs. Furthermore, the lack of expression of TL1A on CD11c⁺CD103⁺ cDCs reduced the generation of Csf2-producing RORγt⁺ ILC3s, suggesting that CD11c⁺CD103⁺ cDCs are critical for producing TL1A, which controls the generation of Csf2-producing RORγt⁺ ILC3s in the gut. Having demonstrated the impaired establishment of oral tolerance and generation of Ag-specific CD4⁺Foxp3⁺pT_{reg} cells under the deficiency of TL1A on CD11c⁺CD103⁺ cDCs as well as antibiotic-driven infant intestinal dysbiotic conditions, our observations support the

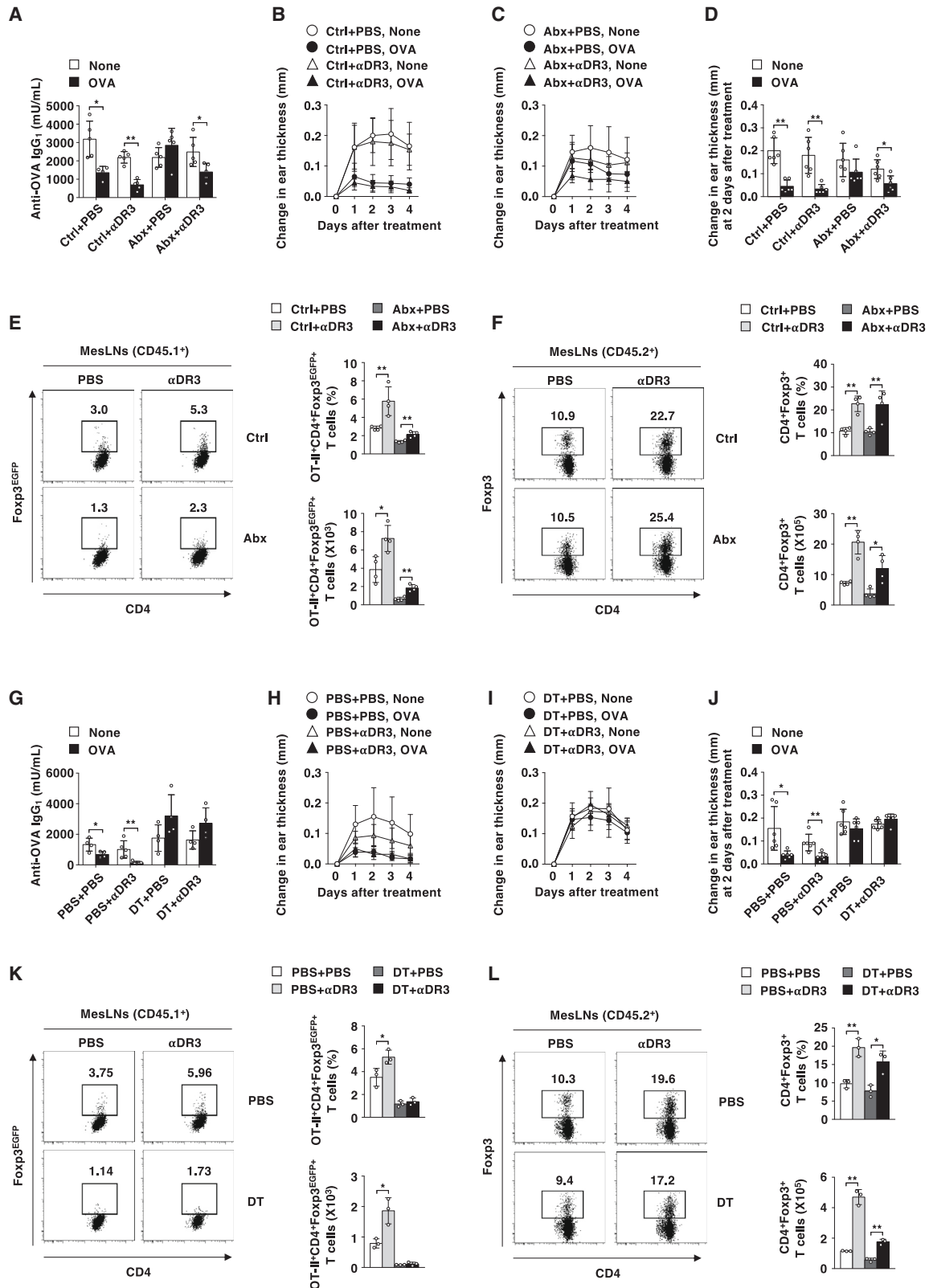
hypothesis that intestinal CD11c⁺CD103⁺ cDCs might sense signals from the gut microbiota to produce TL1A and activate RORγt⁺ ILC3s to secrete Csf2 to maintain the tolerogenesis of CD11c⁺CD103⁺ cDCs for the generation of Ag-specific CD4⁺Foxp3⁺pT_{reg} cells in the interfollicular area in MesLNs in the process of establishing oral tolerance.

In line with the reduced productions of Csf2 and TL1A in MesLNs upon oral combinatorial antibiotic treatment, it reduced the secretion of Csf2 from RORγt⁺ ILC3s and TL1A from CD11c⁺CD103⁺ cDCs. Furthermore, the overexpression of Csf2 or excessive secretion of Csf2 from RORγt⁺ ILC3s upon activation of signaling through DR3 not only restored the defective tolerogenic features of MesLN CD11c⁺CD103⁺ cDCs but also amplified their impaired capacity to generate Ag-specific CD4⁺Foxp3⁺pT_{reg} cells in antibiotic-driven dysbiotic mice. These phenomena suggest that the antibiotic-driven intestinal dysbiosis might reduce the secretion of TL1A from CD11c⁺CD103⁺ cDCs, possibly due to insufficient amounts of pathogen-associated molecular patterns (PAMPs), and might limit the activation of RORγt⁺ ILC3s to produce Csf2 in MesLNs. Furthermore, the reduced production of RORγt⁺ ILC3-derived Csf2 under antibiotic-driven infant intestinal dysbiotic conditions might impair the tolerogenic features of CD11c⁺CD103⁺ cDCs in MesLNs to favor the program in the context of the B7 family of coinhibitory molecules/TGF-β/RA for the generation of CD4⁺Foxp3⁺pT_{reg} cells, leading to the breakdown of oral tolerance. Collectively, our results suggest that the physiological feedback loop between CD11c⁺CD103⁺ cDCs and RORγt⁺ ILC3s in the context of TL1A and Csf2 in MesLNs is critical for the maintenance of tolerogenesis of CD11c⁺CD103⁺ cDCs to establish oral tolerance, whereas antibiotic-driven intestinal dysbiosis destroys the regulatory loop, resulting in the breakdown of oral tolerance.

Having demonstrated the improvement of the dysregulated tolerogenic function of MesLN CD11c⁺CD103⁺ cDCs by RORγt⁺ ILC3-derived Csf2 upon activation of signaling through DR3, the administration of agonistic anti-DR3 mAb not only overcame the impaired induction of oral tolerance but also enhanced the generation of Ag-specific CD4⁺Foxp3⁺pT_{reg} cells in MesLNs in antibiotic-driven dysbiotic mice, whereas they were severely diminished in the absence of CD11c⁺CD103⁺ cDCs. Taken together, these results suggest that the application of agonistic anti-DR3 mAb as a surrogate of TL1A amplifies the Csf2-dependent crosstalk between CD11c⁺CD103⁺ cDCs and RORγt⁺ ILC3s to restore the dysregulated tolerogenic function of

Figure 6. Agonistic anti-DR3 mAb restores the dysregulated tolerogenic function of MesLN CD11c⁺CD103⁺ cDCs in antibiotic-driven dysbiotic mice

(A) Intracellular cytokine expression profile (left panel) and proportion (right panel) of Csf2-producing cells among RORγt⁺ ILC3s in MesLNs.
 (B) Proportion of Csf2⁺ cells among leukocytes in MesLNs.
 (C and D) Cell surface expression profile of ALDEFLUOR⁺ cells among resident I-A/I-E^{hi}CD11c^{hi} cDCs (C) and migratory I-A/I-E^{hi}CD11c⁺ cDCs (D) in MesLNs.
 (E) Proportion of ALDEFLUOR⁺ cells in resident I-A/I-E^{hi}CD11c^{hi} cDCs and migratory I-A/I-E^{hi}CD11c⁺ cDCs (left panel) and their MFI of ALDEFLUOR (right panel) in MesLNs.
 (F) MFI of ALDEFLUOR in cDC subset in MesLNs.
 (G–I) Cell surface expression profile (left panel) and proportion (right panel) of CD45.1⁺OT-II⁺CD4⁺Foxp3^{EGFP+} T cells generated from CD45.1⁺OT-II⁺CD4⁺Foxp3^{EGFP-} T cells cultured with cDCs in the absence (G) or presence of the active (H) or latent (I) form of TGF-β.
 Data were obtained from three to five individual samples in a single experiment of at least three independent experiments. The data are shown from all pooled experiments. The p values are determined by unpaired two-tailed Student's t test. *p < 0.05, **p < 0.01.



(legend on next page)

CD11c⁺CD103⁺ cDCs to generate Ag-specific CD4⁺Foxp3⁺ pT_{reg} cells in MesLNs to establish oral tolerance under antibiotic-driven infant intestinal dysbiotic conditions.

The oral combinatorial antibiotic exposure had multifaceted effects on the tolerogenic features of CD11c⁺ cDC subsets in MesLNs compared with those in SiLPs, while the inducible excessive production of Csf2 led to a more potent enhancement of the tolerogenic features of CD11c⁺ cDC subsets in MesLNs than those in SiLPs. Thus, these observations suggest that CD11c⁺ cDC subsets in MesLNs show greater susceptibility to Csf2 for the maintenance of their tolerogenic features than those in SiLP, possibly due to their prominent expression of Csf2R β . Collectively, the antibiotic-driven infant intestinal dysbiotic conditions could lead to a marked dysregulation of the Csf2-dependent maintenance of tolerogenic features of CD11c⁺ cDCs in MesLNs more than those in SiLPs in the process of the breakdown of oral tolerance.

In conclusion, our findings suggest that CD11c⁺CD103⁺ cDCs are a prerequisite for the establishment of oral tolerance, in which commensal microbes promote crosstalk between CD11c⁺CD103⁺ cDCs and ROR γ t⁺ ILC3s in the milieu of TL1A and Csf2 in MesLNs that provide tolerogenicity in CD11c⁺CD103⁺ cDCs. Furthermore, the antibiotic-driven intestinal dysbiosis dampens their homeostatic feedback loop, leading to the impaired tolerogenic function of CD11c⁺CD103⁺ cDCs, resulting in the failure to establish oral tolerance. Having demonstrated the effective use of agonistic anti-DR3 mAb for improvement of the abortive establishment of oral tolerance, the TL1A-DR3-Csf2 axis may constitute an attractive potential target for intervention and treatment for allergic diseases as well as intestinal inflammatory disorders by acting on the induction of oral tolerance.

Limitations of the study

(1) This study focuses on the requirement of CD11c⁺CD103⁺ cDCs for the induction of oral tolerance. However, the roles of CD11c⁺CD103⁺CD11b⁻ cDCs and CD11c⁺CD103⁺CD11b⁺ cDCs in this process are not yet fully clarified. (2) Our study shows the data linking the reduced expression of Csf2 on ROR γ t⁺ ILC3s to the failed establishment of oral tolerance under antibiotic-driven gut dysbiotic conditions or the absence of CD11c⁺CD103⁺ cDCs. However, the significance of ROR γ t⁺ ILC3s and their production of Csf2 in the establishment of oral tolerance has not been addressed. (3) The use of mixed BM chimeric mice with the deficiency of TL1A and the depletion of CD11c⁺CD103⁺ cDCs could not definitively explore the role of TL1A expressed on CD11c⁺CD103⁺ cDCs in the development of oral tolerance.

STAR★METHODS

Detailed methods are provided in the online version of this paper and include the following:

- KEY RESOURCES TABLE
- RESOURCE AVAILABILITY
 - Lead contact
 - Materials availability
 - Data and code availability
- EXPERIMENTAL MODEL AND SUBJECT DETAILS
 - Mice
- METHOD DETAILS
 - Generation of CD11c:CD103-DTR mice
 - Generation of *Tl1a*^{-/-} mice
 - Cell isolation
 - BM chimeric mice and DT treatment
 - Flow cytometry
 - Quantitative reverse transcription polymerase chain reaction (RT-PCR)
 - *In vitro* CD4⁺ T cell differentiation assay
 - Induction of oral tolerance and immunization with OVA
 - Measurement of serum Flt3L
 - Measurement of serum OVA-specific Ab
 - DTH
 - Airway inflammation in response to OVA
 - Adoptive transfer
 - Histopathologic assessment
 - Immunohistochemical analysis
 - Antibiotic treatment
 - Tumor transplantation for overexpression of Csf2
 - Agonistic anti-DR3 mAb administration
 - 16S rDNA sample acquisition, quantification, and analysis of 16S rDNA
- QUANTIFICATION AND STATISTICAL ANALYSIS

SUPPLEMENTAL INFORMATION

Supplemental information can be found online at <https://doi.org/10.1016/j.celrep.2023.112431>.

ACKNOWLEDGMENTS

We thank all members of the animal facility at University of Miyazaki, Yumiko Sato and Rumi Sunachi for secretarial assistance, and Yukari Kawagoe for technical help in cell sorting. This work was supported by Grants-in-Aid for Scientific Research (B) (K.S., 22H02924) and for Scientific Research (C) (T.U., 20K07703; H.T., 21K07245) from the Ministry of Education, Science and Culture of Japan, the Project for Cancer Research and

Figure 7. Administration of agonistic anti-DR3 mAb affects establishment of oral tolerance in antibiotic-driven dysbiotic mice

(A) Serum level of OVA-specific IgG₁.

(B–D) OVA-specific DTH indicated as ear thickness.

(E and F) Cell surface expression profile (left panel), proportion (top right panel), and absolute number (bottom right panel) of CD45.1⁺OT-II CD4⁺Foxp3^{EGFP+} T cells (E) or aboriginal CD45.2⁺CD4⁺Foxp3⁺ T cells (F) in MesLNs.

(G) Serum level of OVA-specific IgG₁.

(H–J) OVA-specific DTH indicated as ear thickness.

(K and L) Cell surface expression profile (left panel), proportion (top right panel), and absolute number (bottom right panel) of CD45.1⁺OT-II CD4⁺Foxp3^{EGFP+} T cells (K) or aboriginal CD45.2⁺CD4⁺Foxp3⁺ T cells (L) in MesLNs.

Data were obtained from three to six individual samples in a single experiment of at least three independent experiments. The data are shown from all pooled experiments. The p values are determined by unpaired two-tailed Student's t test. *p < 0.05, **p < 0.01.

Therapeutic Evolution (P-CREATE) (K.S., 16cm0106307h0001, 17cm0106307h0002, 18cm0106307h0003, 19cm0106307h0004, 20cm0106307h0005, and 21cm0106307h0006), and the Project for Promotion of Cancer Research and Therapeutic Evolution (P-PROMOTE) (K.S., 22ama221311h0001) from Japan Agency for Medical Research and Development (AMED); Takeda Science Foundation (T.U. and T.F.); GSK Japan Research Grant 2016 (T.F.); and Nipponham Foundation for the Future of Food (H.T. and T.F.).

AUTHOR CONTRIBUTIONS

K.S. designed all experiments, analyzed data, and wrote the manuscript; T.F., T.U., S.M., H.T., Y.N., M.T., and N.C. performed experiments; and Y.H. provided reagents and information.

DECLARATION OF INTERESTS

The authors declare no competing interests.

Received: October 31, 2021

Revised: February 21, 2023

Accepted: April 10, 2023

REFERENCES

- Guilliams, M., Ginhoux, F., Jakubczak, C., Naik, S.H., Onai, N., Schraml, B.U., Segura, E., Tussiwand, R., and Yona, S. (2014). Dendritic cells, monocytes and macrophages: a unified nomenclature based on ontogeny. *Nat. Rev. Immunol.* *14*, 571–578 <https://pubmed.ncbi.nlm.nih.gov/25033907>.
- Murphy, T.L., Grajales-Reyes, G.E., Wu, X., Tussiwand, R., Briseño, C.G., Iwata, A., Kretzer, N.M., Durai, V., and Murphy, K.M. (2016). Transcriptional control of dendritic cell development. *Annu. Rev. Immunol.* *34*, 93–119 <https://pubmed.ncbi.nlm.nih.gov/26735697>.
- Sato, K., Uto, T., Fukaya, T., and Takagi, H. (2017). Regulatory dendritic cells. *Curr. Top. Microbiol. Immunol.* *410*, 47–71 <https://pubmed.ncbi.nlm.nih.gov/28900681>.
- Uto, T., Takagi, H., Fukaya, T., Nasu, J., Fukui, T., Miyayama, N., Arimura, K., Nakamura, T., Chojookhuu, N., Hishikawa, Y., and Sato, K. (2018). Critical role of plasmacytoid dendritic cells in induction of oral tolerance. *J. Allergy Clin. Immunol.* *141*, 2156–2167.e9 <https://pubmed.ncbi.nlm.nih.gov/29477579>.
- Honda, K., and Littman, D.R. (2016). The microbiota in adaptive immune homeostasis and disease. *Nature* *535*, 75–84. <https://pubmed.ncbi.nlm.nih.gov/27383982>.
- Bekiaris, V., Persson, E.K., and Agace, W.W. (2014). Intestinal dendritic cells in the regulation of mucosal immunity. *Immunol. Rev.* *260*, 86–101 <https://pubmed.ncbi.nlm.nih.gov/24942684>.
- Fukaya, T., Takagi, H., Sato, Y., Sato, K., Eizumi, K., Taya, H., Shin, T., Chen, L., Dong, C., Azuma, M., et al. (2010). Crucial roles of B7-H1 and B7-DC expressed on mesenteric lymph node dendritic cells in the generation of antigen-specific CD4⁺Foxp3⁺ regulatory T cells in the establishment of oral tolerance. *Blood* *116*, 2266–2276. <https://pubmed.ncbi.nlm.nih.gov/20574047>.
- Esterházy, D., Loschko, J., London, M., Jove, V., Oliveira, T.Y., and Mucida, D. (2016). Classical dendritic cells are required for dietary antigen-mediated induction of peripheral T_{reg} cells and tolerance. *Nat. Immunol.* *17*, 545–555 <https://pubmed.ncbi.nlm.nih.gov/27019226>.
- Rescigno, M. (2011). Dendritic cells in oral tolerance in the gut. *Cell Microbiol.* *13*, 1312–1318 <https://pubmed.ncbi.nlm.nih.gov/21740494>.
- Mazzini, E., Massimiliano, L., Penna, G., and Rescigno, M. (2014). Oral tolerance can be established via gap junction transfer of fed antigens from CX3CR1⁺ macrophages to CD103⁺ dendritic cells. *Immunity* *40*, 248–261. <https://pubmed.ncbi.nlm.nih.gov/24462723>.
- Veenbergen, S., van Berkel, L.A., du Pré, M.F., He, J., Karrich, J.J., Costes, L.M.M., Luk, F., Simons-Oosterhuis, Y., Raatgeep, H.C., Cerovic, V., et al. (2016). Colonic tolerance develops in the iliac lymph nodes and can be established independent of CD103⁺ dendritic cells. *Mucosal Immunol.* *9*, 894–906 <https://pubmed.ncbi.nlm.nih.gov/26577569>.
- Shiokawa, A., Kotaki, R., Takano, T., Nakajima-Adachi, H., and Hachimura, S. (2017). Mesenteric lymph node CD11b⁺ CD103⁺ PD-L1^{high} dendritic cells highly induce regulatory T cells. *Immunology* *152*, 52–64. <https://pubmed.ncbi.nlm.nih.gov/28423181>.
- Stagg, A.J. (2018). Intestinal dendritic cells in health and gut inflammation. *Front. Immunol.* *9*, 2883 <https://pubmed.ncbi.nlm.nih.gov/30574151>.
- Miyayama, N., Takagi, H., Uto, T., Fukaya, T., Nasu, J., Fukui, T., Nishikawa, Y., Sparwasser, T., Chojookhuu, N., Hishikawa, Y., et al. (2020). Essential role of submandibular lymph node dendritic cells in protective sublingual immunotherapy against murine allergy. *Commun. Biol.* *3*, 742 <https://pubmed.ncbi.nlm.nih.gov/33288832>.
- Owen, J.L., and Mohamadzadeh, M. (2013). Microbial activation of gut dendritic cells and the control of mucosal immunity. *J. Interferon Cytokine Res.* *33*, 619–631 <https://pubmed.ncbi.nlm.nih.gov/23962004>.
- Frank, D.N., St Amand, A.L., Feldman, R.A., Boedeker, E.C., Harpaz, N., and Pace, N.R. (2007). Molecular-phylogenetic characterization of microbial community imbalances in human inflammatory bowel diseases. *Proc. Natl. Acad. Sci. USA* *104*, 13780–13785. <https://pubmed.ncbi.nlm.nih.gov/17699621>.
- Round, J.L., O'Connell, R.M., and Mazmanian, S.K. (2010). Coordination of tolerogenic immune responses by the commensal microbiota. *J. Autoimmun.* *34*, J220–J225 <https://pubmed.ncbi.nlm.nih.gov/19963349>.
- McKenzie, C., Tan, J., Macia, L., and Mackay, C.R. (2017). The nutrition-gut microbiome-physiology axis and allergic diseases. *Immunol. Rev.* *278*, 277–295 <https://pubmed.ncbi.nlm.nih.gov/28658542>.
- Hill, D.A., Siracusa, M.C., Abt, M.C., Kim, B.S., Kobuley, D., Kubo, M., Kambayashi, T., Larosa, D.F., Renner, E.D., Orange, J.S., et al. (2012). Commensal bacteria-derived signals regulate basophil hematopoiesis and allergic inflammation. *Nat. Med.* *18*, 538–546 <https://pubmed.ncbi.nlm.nih.gov/22447074>.
- Russell, S.L., Gold, M.J., Hartmann, M., Willing, B.P., Thorson, L., Wlodarska, M., Gill, N., Blanchet, M.R., Mohn, W.W., McNagny, K.M., and Finlay, B.B. (2012). Early life antibiotic-driven changes in microbiota enhance susceptibility to allergic asthma. *EMBO Rep.* *13*, 440–447 <https://pubmed.ncbi.nlm.nih.gov/22422004>.
- Stefka, A.T., Feehley, T., Tripathi, P., Qiu, J., McCoy, K., Mazmanian, S.K., Tjota, M.Y., Seo, G.Y., Cao, S., Theriault, B.R., et al. (2014). Commensal bacteria protect against food allergen sensitization. *Proc. Natl. Acad. Sci. USA* *111*, 13145–13150. <https://pubmed.ncbi.nlm.nih.gov/25157157>.
- Huang, C., Wang, J., Zheng, X., Chen, Y., Zhou, R., Wei, H., Sun, R., and Tian, Z. (2018). Commensal bacteria aggravate allergic asthma via NLRP3/IL-1 β signaling in post-weaning mice. *J. Autoimmun.* *93*, 104–113 <https://pubmed.ncbi.nlm.nih.gov/30146006>.
- Arrieta, M.C., Stiersma, L.T., Amenogbe, N., Brown, E.M., and Finlay, B. (2014). The intestinal microbiome in early life: health and disease. *Front. Immunol.* *5*, 427 <https://pubmed.ncbi.nlm.nih.gov/25250028>.
- Arrieta, M.C., Sadarangani, M., Brown, E.M., Russell, S.L., Nimmo, M., Dean, J., Turvey, S.E., Chan, E.S., and Finlay, B.B. (2016). A humanized microbiota mouse model of ovalbumin-induced lung inflammation. *Gut Microb.* *7*, 342–352 <https://pubmed.ncbi.nlm.nih.gov/27115049>.
- Sudo, N., Sawamura, S., Tanaka, K., Aiba, Y., Kubo, C., and Koga, Y. (1997). The requirement of intestinal bacterial flora for the development of an IgE production system fully susceptible to oral tolerance induction. *J. Immunol.* *159*, 1739–1745 <https://pubmed.ncbi.nlm.nih.gov/9257835>.
- Maeda, Y., Noda, S., Tanaka, K., Sawamura, S., Aiba, Y., Ishikawa, H., Hasegawa, H., Kawabe, N., Miyasaka, M., and Koga, Y. (2001). The failure of oral tolerance induction is functionally coupled to the absence of T cells in

- Peyer's patches under germfree conditions. *Immunobiology* 204, 442–457. <https://pubmed.ncbi.nlm.nih.gov/11776399>.
27. Ishikawa, H., Tanaka, K., Maeda, Y., Aiba, Y., Hata, A., Tsuji, N.M., Koga, Y., and Matsumoto, T. (2008). Effect of intestinal microbiota on the induction of regulatory CD25⁺CD4⁺ T cells. *Clin. Exp. Immunol.* 153, 127–135 <https://pubmed.ncbi.nlm.nih.gov/18460018>.
 28. Haciní-Rachinel, F., Gomez de Agüero, M., Kanjarawi, R., Moro-Sibilot, L., Le Ludeuc, J.B., Macari, C., Boschetti, G., Bardel, E., Langella, P., Dubois, B., and Kaiserlian, D. (2018). Intestinal dendritic cell licensing through Toll-like receptor 4 is required for oral tolerance in allergic contact dermatitis. *J. Allergy Clin. Immunol.* 141, 163–170 <https://pubmed.ncbi.nlm.nih.gov/28342908>.
 29. Nutten, S., Schumann, A., Donnicola, D., Mercenier, A., Rami, S., and Garcia-Rodenas, C.L. (2007). Antibiotic administration early in life impairs specific humoral responses to an oral antigen and increases intestinal mast cell numbers and mediator concentrations. *Clin. Vaccine Immunol.* 14, 190–197 <https://pubmed.ncbi.nlm.nih.gov/17151185>.
 30. Lambert, S.E., Kinder, J.M., Then, J.E., Parliament, K.N., and Bruns, H.A. (2012). Erythromycin treatment hinders the induction of oral tolerance to fed ovalbumin. *Front. Immunol.* 3, 203 <https://pubmed.ncbi.nlm.nih.gov/22826710>.
 31. Kim, M., Galan, C., Hill, A.A., Wu, W.J., Fehlner-Peach, H., Song, H.W., Schady, D., Bettini, M.L., Simpson, K.W., Longman, R.S., et al. (2018). Critical role for the microbiota in CX3CR1⁺ intestinal mononuclear phagocyte regulation of intestinal T cell responses. *Immunity* 49, 151–163.e5. <https://pubmed.ncbi.nlm.nih.gov/29980437>.
 32. Durai, V., and Murphy, K.M. (2016). Functions of murine dendritic cells. *Immunity* 45, 719–736. <https://pubmed.ncbi.nlm.nih.gov/27760337>.
 33. Caton, M.L., Smith-Raska, M.R., and Reizis, B. (2007). Notch-RBP-J signaling controls the homeostasis of CD8⁺ dendritic cells in the spleen. *J. Exp. Med.* 204, 1653–1664 <https://pubmed.ncbi.nlm.nih.gov/17591855>.
 34. Jung, S., Unutmaz, D., Wong, P., Sano, G.I., De los Santos, K., Sparwasser, T., Wu, S., Vuthoori, S., Ko, K., Zavala, F., et al. (2002). In vivo depletion of CD11c⁺ dendritic cells abrogates priming of CD8⁺ T cells by exogenous cell-associated antigens. *Immunity* 17, 211–220. <https://pubmed.ncbi.nlm.nih.gov/12196292>.
 35. Fukaya, T., Murakami, R., Takagi, H., Sato, K., Sato, Y., Otsuka, H., Ohno, M., Hijikata, A., Ohara, O., Hikida, M., et al. (2012). Conditional ablation of CD205⁺ conventional dendritic cells impacts the regulation of T cell immunity and homeostasis in vivo. *Proc. Natl. Acad. Sci. USA* 109, 11288–11293. <https://pubmed.ncbi.nlm.nih.gov/22736794>.
 36. Takagi, H., Fukaya, T., Eizumi, K., Sato, Y., Sato, K., Shibazaki, A., Otsuka, H., Hijikata, A., Watanabe, T., Ohara, O., et al. (2011). Plasmacytoid dendritic cells are crucial for the initiation of inflammation and T cell immunity in vivo. *Immunity* 35, 958–971. <https://pubmed.ncbi.nlm.nih.gov/22177923>.
 37. Uto, T., Fukaya, T., Takagi, H., Arimura, K., Nakamura, T., Kojima, N., Malissen, B., and Sato, K. (2016). Clec4A4 is a regulatory receptor for dendritic cells that impairs inflammation and T-cell immunity. *Nat. Commun.* 7, 11273 <https://pubmed.ncbi.nlm.nih.gov/27068492>.
 38. Esterházy, D., Canesso, M.C.C., Mesin, L., Muller, P.A., de Castro, T.B.R., Lockhart, A., ElJalby, M., Faria, A.M.C., and Mucida, D. (2019). Compartmentalized gut lymph node drainage dictates adaptive immune responses. *Nature* 569, 126–130. <https://pubmed.ncbi.nlm.nih.gov/30988509>.
 39. Atarashi, K., Tanoue, T., Shima, T., Imaoka, A., Kuwahara, T., Momose, Y., Cheng, G., Yamasaki, S., Saito, T., Ohba, Y., et al. (2011). Induction of colonic regulatory T cells by indigenous Clostridium species. *Science* 331, 337–341. <https://pubmed.ncbi.nlm.nih.gov/21205640>.
 40. Walton, K.L.W., He, J., Kelsall, B.L., Sartor, R.B., and Fisher, N.C. (2006). Dendritic cells in germ-free and specific pathogen-free mice have similar phenotypes and in vitro antigen presenting function. *Immunol. Lett.* 102, 16–24 <https://pubmed.ncbi.nlm.nih.gov/16105690>.
 41. Hägerbrand, K., Westlund, J., Yrlid, U., Agace, W., and Johansson-Lindbom, B. (2015). MyD88 signaling regulates steady-state migration of intestinal CD103⁺ dendritic cells independently of TNF- α and the gut microbiota. *J. Immunol.* 195, 2888–2899 <https://pubmed.ncbi.nlm.nih.gov/26259586>.
 42. Mortha, A., Chudnovskiy, A., Hashimoto, D., Bogunovic, M., Spencer, S.P., Belkaid, Y., and Merad, M. (2014). Microbiota-dependent crosstalk between macrophages and ILC3 promotes intestinal homeostasis. *Science* 343, 1249288. <https://pubmed.ncbi.nlm.nih.gov/24625929>.
 43. Mackley, E.C., Houston, S., Marriott, C.L., Halford, E.E., Lucas, B., Cerovic, V., Filbey, K.J., Maizels, R.M., Hepworth, M.R., Sonnenberg, G.F., et al. (2015). CCR7-dependent trafficking of ROR γ ⁺ ILCs creates a unique microenvironment within mucosal draining lymph nodes. *Nat. Commun.* 6, 5862 <https://pubmed.ncbi.nlm.nih.gov/25575242>.
 44. Castellanos, J.G., Woo, V., Viladomiu, M., Putzel, G., Lima, S., Diehl, G.E., Marderstein, A.R., Gandara, J., Perez, A.R., Withers, D.R., et al. (2018). Microbiota induced TNF-like ligand 1A drives group 3 innate lymphoid cell-mediated barrier protection and intestinal T cell activation during colitis. *Immunity* 49, 1077–1089.e5. <https://pubmed.ncbi.nlm.nih.gov/30552020>.
 45. Li, J., Shi, W., Sun, H., Ji, Y., Chen, Y., Guo, X., Sheng, H., Shu, J., Zhou, L., Cai, T., and Qiu, J. (2019). Activation of DR3 signaling causes loss of ILC3s and exacerbates intestinal inflammation. *Nat. Commun.* 10, 3371 <https://pubmed.ncbi.nlm.nih.gov/31358760>.
 46. Dranoff, G., Jaffee, E., Lazenby, A., Golumbek, P., Levitsky, H., Brose, K., Jackson, V., Hamada, H., Pardoll, D., and Mulligan, R.C. (1993). Vaccination with irradiated tumor cells engineered to secrete murine granulocyte-macrophage colony-stimulating factor stimulates potent, specific, and long-lasting anti-tumor immunity. *Proc. Natl. Acad. Sci. USA* 90, 3539–3543. <https://pubmed.ncbi.nlm.nih.gov/8097319>.
 47. Kim, B.S., Nishikii, H., Baker, J., Pierini, A., Schneidawind, D., Pan, Y., Beilhack, A., Park, C.G., and Negrin, R.S. (2015). Treatment with agonistic DR3 antibody results in expansion of donor Tregs and reduced graft-versus-host disease. *Blood* 126, 546–557. <https://pubmed.ncbi.nlm.nih.gov/26063163>.
 48. Birnberg, T., Bar-On, L., Sapoznikov, A., Caton, M.L., Cervantes-Barragán, L., Makia, D., Krauthgamer, R., Brenner, O., Ludewig, B., Brockschneider, D., et al. (2008). Lack of conventional dendritic cells is compatible with normal development and T cell homeostasis, but causes myeloid proliferative syndrome. *Immunity* 29, 986–997. <https://pubmed.ncbi.nlm.nih.gov/19062318>.
 49. Fukaya, T., Fukui, T., Uto, T., Takagi, H., Nasu, J., Miyanaga, N., Arimura, K., Nakamura, T., Koseki, H., Chojookhuu, N., et al. (2018). Pivotal role of IL-22 binding protein in the epithelial autoregulation of interleukin-22 signaling in the control of skin inflammation. *Front. Immunol.* 9, 1418 <https://pubmed.ncbi.nlm.nih.gov/29977242>.
 50. Nishikawa, Y., Fukaya, T., Fukui, T., Uto, T., Takagi, H., Nasu, J., Miyanaga, N., Riethmacher, D., Chojookhuu, N., Hishikawa, Y., et al. (2021). Congenital deficiency of conventional dendritic cells promotes the development of atopic dermatitis-like inflammation. *Front. Immunol.* 12, 712676 <https://pubmed.ncbi.nlm.nih.gov/34394115>.
 51. Zhou, L., Chu, C., Teng, F., Bessman, N.J., Goc, J., Santosa, E.K., Putzel, G.G., Kabata, H., Kelsen, J.R., Baldassano, R.N., et al. (2019). Innate lymphoid cells support regulatory T cells in the intestine through interleukin-2. *Nature* 568, 405–409. <https://pubmed.ncbi.nlm.nih.gov/30944470>.
 52. Farley, F.W., Soriano, P., Steffen, L.S., and Dymecki, S.M. (2000). Widespread recombinase expression using FLPeR (Flipper) mice. *Genesis* 28, 106–110. <https://pubmed.ncbi.nlm.nih.gov/11105051>.
 53. Arimura, K., Takagi, H., Uto, T., Fukaya, T., Nakamura, T., Chojookhuu, N., Hishikawa, Y., Yamashita, Y., and Sato, K. (2017). Crucial role of plasmacytoid dendritic cells in the development of acute colitis through the regulation of intestinal inflammation. *Mucosal Immunol.* 10, 957–970 <https://pubmed.ncbi.nlm.nih.gov/27848952>.

STAR★METHODS

KEY RESOURCES TABLE

REAGENT or RESOURCE	SOURCE	IDENTIFIER
Antibodies		
Anti-mouse B7-H1 conjugated to PE (clone MIH5)	BD Biosciences	Cat#558091; RRID: AB_397018
Anti-mouse B7-DC conjugated to PE (clone TY25)	ThermoFisher	Cat#12-5986-82; RRID: AB_466097
Anti-mouse CD3 unconjugated (clone SP7)	Abcam	Cat# ab16669; RRID: AB_443425
Anti-mouse CD3 ϵ conjugated to BV510 (clone 145-2C11)	BD Biosciences	Cat#563024; RRID: AB_2737959
Anti-mouse CD3 ϵ conjugated to PE (clone 145-2C11)	BioLegend	Cat#100308; RRID: AB_312673
Anti-mouse CD3 ϵ conjugated to PerCP-Cy5.5 (clone 145-2C11)	BioLegend	Cat#100328; RRID: AB_893318
Anti-mouse CD3 ϵ conjugated to APC (clone 145-2C11)	BioLegend	Cat#100312; RRID: AB_312677
Anti-mouse CD3 ϵ conjugated to APC (clone KT3.1.1)	BioLegend	Cat#155606; RRID: AB_2750432
Anti-mouse CD4 conjugated to PE (clone RM4-5)	BD Biosciences	Cat#553048; RRID: AB_394584
Anti-mouse CD4 conjugated to PE-Cy7 (clone RM4-5)	BD Biosciences	Cat#561099; RRID: AB_2034007
Anti-mouse CD8 α conjugated to FITC (clone 53-6.7)	BD Biosciences	Cat#553030; RRID: AB_394568
Anti-mouse CD8 α conjugated to APC (clone 53-6.7)	BD Biosciences	Cat#561093; RRID: AB_10563416
Anti-mouse CD8 α conjugated to APC-Cy7 (clone 53-6.7)	BioLegend	Cat#100714; RRID: AB_312753
Anti-mouse CD11b conjugated to PE-Cy7 (clone M1/70)	BD Biosciences	Cat#561098; RRID: AB_2033994
Anti-mouse CD11c conjugated to FITC (clone HL3)	BD Biosciences	Cat#553801; RRID: AB_395060
Anti-mouse CD11c conjugated to APC (clone HL3)	BD Biosciences	Cat#561119; RRID: AB_10562405
Anti-mouse CD11c conjugated to BV421 (clone HL3)	BD Biosciences	Cat#562782; RRID: AB_2737789
Anti-mouse CD11c conjugated to Alexa-488 (clone N418)	BioLegend	Cat#117313; RRID: AB_492849
Anti-mouse CD11c conjugated to Alexa-594 (clone N418)	BioLegend	Cat#117346; RRID: AB_2563323
Anti-mouse CD19 conjugated to PE-eFluor 610 (clone eBio1D3)	ThermoFisher	Cat#61-0193-82; RRID: AB_2574536
Anti-mouse CD44 conjugated to PE (clone IM7)	BD Biosciences	Cat#561860; RRID: AB_10895375
Anti-mouse CD44 conjugated to APC (clone IM7)	BD Biosciences	Cat#559250; RRID: AB_398661
Anti-mouse CD44 conjugated to BV510 (clone IM7)	BD Biosciences	Cat#563114; RRID: AB_2738011
Anti-mouse CD45 conjugated to APC-Cy7 (clone 30-F11)	BioLegend	Cat#103116; RRID: AB_312981
Anti-mouse CD45R/B220 conjugated to APC (clone RA3-6B2)	BD Biosciences	Cat#561880; RRID: AB_10897020
Anti-mouse CD45R/B220 conjugated to Alexa-488 (clone RA3-6B2)	BD Biosciences	Cat#557669; RRID: AB_396781
Anti-mouse CD45R/B220 conjugated to PE-Cy7 (clone RA3-6B2)	BioLegend	Cat#103222; RRID: AB_313005
Anti-mouse CD45R/B220 conjugated to APC-Cy7 (clone RA3-6B2)	BioLegend	Cat#103224; RRID: AB_313007
Anti-mouse CD45RB conjugated to PE (clone 16A)	BD Biosciences	Cat#553101; RRID: AB_394627
Anti-mouse CD45.1 conjugated to FITC (clone A20)	BD Biosciences	Cat#553775; RRID: AB_395043
Anti-mouse CD45.1 conjugated to APC (clone A20)	BD Biosciences	Cat#558701; RRID: AB_1645214
Anti-mouse CD45.1 conjugated to BV421 (clone A20)	BD Biosciences	Cat#563983; RRID: AB_2738523
Anti-mouse CD45.1 conjugated to PE-Cy7 (clone A20)	BioLegend	Cat#110730; RRID: AB_1134168
Anti-mouse CD45.1 conjugated to APC-Cy7 (clone A20)	BioLegend	Cat#110716; RRID: AB_313505
Anti-mouse CD45.2 conjugated to APC-Cy7 (clone 104)	BioLegend	Cat#109824; RRID: AB_830789
Anti-mouse CD62L conjugated to FITC (clone MEL-14)	BD Biosciences	Cat#553150; RRID: AB_394665

(Continued on next page)

Continued

REAGENT or RESOURCE	SOURCE	IDENTIFIER
Anti-mouse CD62L conjugated to BV421 (clone MEL-14)	BD Biosciences	Cat#562910; RRID: AB_2737885
Anti-mouse CD64 conjugated to PE (clone X54-5/7.1)	BioLegend	Cat#139304; RRID: AB_10612740
Anti-mouse CD64 conjugated to APC (clone X54-5/7.1)	BioLegend	Cat#139306; RRID: AB_11219391
Anti-mouse CD80 conjugated to APC (clone 16-10A1)	BioLegend	Cat#104714; RRID: AB_313135
Anti-mouse CD86 conjugated to APC (clone GL-1)	BioLegend	Cat#105012; RRID: AB_493342
Anti-mouse CD103 conjugated to PE (clone M290)	BD Biosciences	Cat#557495; RRID: AB_396732
Anti-mouse CD103 conjugated to BV421 (clone M290)	BD Biosciences	Cat#566297; RRID: AB_2739670
Anti-mouse CD103 conjugated to Alexa-647 (clone 2E7)	BioLegend	Cat#121409; RRID: AB_535951
Anti-mouse CD127 conjugated to PE (clone A7R34)	BioLegend	Cat#135009; RRID: AB_1937252
Anti-mouse CD131 conjugated to APC (clone REA193)	Miltenyi Biotec	Cat# 130-102-536; RRID: AB_2654864
Anti-mouse CX3CR1 conjugated to Alexa-488 (clone SA011F11)	BioLegend	Cat#149021; RRID: AB_2565704
Anti-mouse DR3 conjugated to APC (clone 4C12)	BioLegend	Cat#144407; RRID: AB_2687247
Anti-mouse Foxp3 conjugated to APC (clone FJK-16s)	ThermoFisher	Cat#17-5773-82; RRID: AB_469457
Anti-mouse Foxp3 conjugated to Alexa-488 (clone MF-14)	BioLegend	Cat#126405; RRID: AB_1089114
Anti-mouse F4/80 conjugated to PE (clone BM8)	BioLegend	Cat#123109; RRID: AB_893498
Anti-mouse GM-CSF conjugated to APC (clone MP1-22E9)	BioLegend	Cat#505413; RRID: AB_2721460
Anti-mouse GM-CSF R alpha conjugated to APC (clone 698423)	R&D Systems	Cat#FAB6130A; RRID: AB_10973836
Anti-mouse I-A/I-E conjugated to APC-Cy7 (clone M5/114.15.2)	BioLegend	Cat#107628; RRID: AB_2069377
Anti-mouse I-A/I-E conjugated to BV510 (clone M5/114.15.2)	BioLegend	Cat#107636; RRID: AB_2734168
Anti-mouse Ly6C conjugated to APC (clone HK1.4)	BioLegend	Cat#128015; RRID: AB_1732087
Anti-mouse Ly6G conjugated to FITC (clone 1A8)	BioLegend	Cat#127605; RRID: AB_1236488
Anti-mouse NK1.1 conjugated to FITC (clone PK136)	BD Biosciences	Cat#553164; RRID: AB_394676
Anti-mouse ROR γ t conjugated to BV421 (clone Q31-378)	BD Biosciences	Cat#562894; RRID: AB_2687545
Anti-mouse ROR γ t unconjugated (clone AFKJS-9)	eBioscience	Cat#14-6988-82; RRID: AB_1834475
Anti-mouse Siglec-F conjugated to PE (clone REA798)	Miltenyi Biotec	Cat#130-112-332; RRID: AB_2653439
Anti-mouse Siglec-H conjugated to PE (clone 551)	BioLegend	Cat#129605; RRID: AB_1227763
Anti-mouse TCR γ/δ conjugated to PE (clone GL3)	BioLegend	Cat#118107; RRID: AB_313831
Anti-mouse TL1A conjugated to PerCP-eFluor 710 (clone Tandys1a)	ThermoFisher	Cat#46-7911-82; RRID: AB_11217878
Goat anti-rabbit Immunoglobulins conjugated to HRP (polyclonal)	Dako	Cat#P0448; RRID: AB_2617138
Goat anti-rat IgG conjugated to HRP (polyclonal)	Millipore	Cat#AP136P; RRID: AB_91300
Mouse IgG, kappa isotype control conjugated to PerCP-eFluor 710 (clone P3.6.2.8.1)	ThermoFisher	Cat#46-4714-82; RRID: AB_1834453
Ultra-LEAF TM Purified anti-mouse DR3 (clone 4C12)	BioLegend	Cat# 144412; RRID: AB_2800672

Chemicals, peptides, and recombinant proteins

Collagenase type III	Worthington Biochemical	Cat#CLS-3
RBC Lysis buffer	Sigma-Aldrich	Cat#R7757-100ML
Paraformaldehyde	Wako Pure Chemicals	Cat#163-20145
Paraffin	Fujifilm	Cat#162-18961

(Continued on next page)

Continued

REAGENT or RESOURCE	SOURCE	IDENTIFIER
Mayer's Hematoxylin Solution	Fujifilm	Cat#131-09665
Eosin Alcohol Solution	Fujifilm	Cat#050-06041
IgG from goat serum	Sigma-Aldrich	Cat#I9140
Brij L23	Sigma-Aldrich	Cat#B4184
SlowFade Diamond Antifade Mountant	Invitrogen	Cat#S36963
Percoll	GE Healthcare	Cat#17-0891-01
Dispase	BD Biosciences	Cat#354235
DNase I	Roche	Cat#11284932001
DAPI	Invitrogen	Cat#D1306
Phorbol 12-myristate 13-acetate (PMA)	Sigma-Aldrich	Cat#8139-1MG
Ionomycin	Sigma-Aldrich	Cat#10634-1MG
Brefeldin A solution	eBioscience	Cat#00-4506
Recombinant human TGF- β 1	Wako Pure Chemicals	Cat#209-16544
Recombinant Human Latent TGF- β 1	R&D Systems	Cat#299-LT
Recombinant mouse GM-CSF	Wako Pure Chemicals	Cat#077-04674
Diphtheria Toxin from <i>Corynebacterium diphtheriae</i>	Sigma-Aldrich	Cat#D0564-1MG
Propidium iodide	Sigma-Aldrich	Cat#P4170-25MG
Albumin from chicken egg white	Sigma-Aldrich	Cat#A5503
Kanamycin Sulfate	Wako Pure Chemicals	Cat#113-00343
Gentamicin Sulfate	Wako Pure Chemicals	Cat#077-02974
Metronidazole	Wako Pure Chemicals	Cat#132-18061
Colistin Sulfate	Wako Pure Chemicals	Cat#038-20943
Vancomycin Hydrochloride	Wako Pure Chemicals	Cat#226-01306

Critical commercial assays

Mouse CD4 T Lymphocyte Enrichment Set - DM	BD Biosciences	Cat#558131
Mouse CD8 T Lymphocyte Enrichment Set - DM	BD Biosciences	Cat#558471
Mouse CD11c (N418) Microbeads	Miltenyi Biotec	Cat#130-125-835
ALDEFUOR kit	StemCell Technologies	Cat#01700
Fixation-Permeabilization solution Set	eBiosciences	Cat#88-8824-00
Complete Freund Adjuvant	Difco	Cat#263810
Imject Alum Adjuvant	ThermoFisher	Cat#77161
RNeasy plus micro kit	Qiagen	Cat#74034
PrimeScript RT Master Mix	Takara	Cat#RR036A
SYBR® Premix Ex Taq II	Takara	Cat#RR820A
Cell Proliferation Dye eFluor 670	eBioscience	Cat#65-0840-85
BAC Modification Kit, Quick and Easy	Gene Bridges	Cat#K001
LBIS Mouse OVA-IgE ELISA Kit	FUJIFILM Wako Shibayagi	Cat#AKRIE-030
LBIS Mouse OVA-IgG ₁ ELISA Kit	FUJIFILM Wako Shibayagi	Cat#AKRIE-040
5(6)-FAM, SE (5-(and-6)-Carboxyfluorescein, Succinimidyl Ester), mixed isomers	Invitrogen	Cat#C1311
NHS-Rhodamine	Invitrogen	Cat#46406
Mouse/Rat Flt-3 Ligand/FLT3L	R&D Systems	Cat#MFK00
Quantikine ELISA Kit		

Deposited data

Bacterial 16S rRNA sequencing data reported in this study	DNA Data Bank of Japan's BioProject	DRA015912
---	-------------------------------------	-----------

Experimental models: Cell lines

Mouse: B16-F10	RIKEN IMS	N/A
Mouse: B16 ^{C57}	RIKEN BRC	Stock No: RCB1158

(Continued on next page)

REAGENT or RESOURCE	SOURCE	IDENTIFIER
Continued		
Experimental models: Organisms/strains		
Mouse: C57BL/6	Japan Clea	Ordering name: C57BL/6Jcl
Mouse: B6.FLPeR mice	Jackson Laboratory	Stock No: 016226
Mouse: B6.CD11c-Cre mice	Jackson Laboratory	Stock No: 008068
Mouse: B6.CD45.1 OT-I mice	Takagi et al. ³⁶	N/A
Mouse: B6.CD45.1 OT-II mice	Takagi et al. ³⁶	N/A
Mouse: B6.CD45.1 Foxp3 ^{EGFP} OT-II mice	Takagi et al. ³⁶	N/A
Mouse: B6.CD103-LSL-DTR mice	This paper	N/A
Mouse: B6. <i>T11a</i> ^{-/-} mice	This paper	N/A
Oligonucleotides		
<i>Gapdh</i> -F (AAATTCAACGGCACAGTCAAG)	This paper	N/A
<i>Gapdh</i> -R (TGGTGGTGAAGACACCAGTAG)	This paper	N/A
<i>Il1b</i> -F (GAAGAAGAGCCCATCCTCTG)	This paper	N/A
<i>Il1b</i> -R (TCATCTCGGAGCCTGTAGTG)	This paper	N/A
<i>Tnfsf15</i> -F (TCCCATCCTCGCAGGACTTA)	This paper	N/A
<i>Tnfsf15</i> -R (GCTGTGGTGAAGGCTCAGAT)	This paper	N/A
<i>Csf2</i> -F (TCGTCTCTAACGAGTTCTCCTT)	This paper	N/A
<i>Csf2</i> -R (CGTAGACCCTGCTCGAATATCT)	This paper	N/A
<i>Tgfb1</i> -F (ACCATGCCAACTTCTGTCTG)	This paper	N/A
<i>Tgfb1</i> -R (CGGGTTGTGTTGGTTGTAGA)	This paper	N/A
<i>Itgb8</i> -F (ACAGCATCGCATGGACCAA)	This paper	N/A
<i>Itgb8</i> -R (AAGCAACCCGATCAAGAATGTG)	This paper	N/A
<i>Aldh1a2</i> -F (CCTTTGATCCCACAAGTGAACA)	This paper	N/A
<i>Aldh1a2</i> -R (AGCCACACCGCTCTGGATAA)	This paper	N/A
Primer 1: <i>Cd103</i> -BAC-5LR-F (CATTGAAGTATT TAGCATTACAATCCAT)	This paper	N/A
Primer 2: 5LR- <i>Dtr</i> -R (ATAACCTCCTCTC CTATGGTACCTAAAC)	This paper	N/A
Primer 3: 3LR- <i>Dtr</i> -F (GACCTTTTGAGAG TCACTTTATCCTC)	This paper	N/A
Primer 4: <i>Cd103</i> -BAC-3LR-R (ATCTTCT GACAAACTACGACATGTTCCAC)	This paper	N/A
Primer 5: <i>Cd11c</i> - <i>Cre</i> -F (ACTTGGCAGCTGTCTCCAAG)	Caton et al. ³³	N/A
Primer 6: <i>Cd11c</i> - <i>Cre</i> -R (GCGAACATCTTCAGGTTCTG)	Caton et al. ³³	N/A
<i>Tnfsf15</i> -gRNA-A1 (CAG GCTTGAGCACGAGACGCAGG)	This paper	N/A
<i>Tnfsf15</i> -gRNA-A2 (TACCCTAGACCAGTTAGCACTGG)	This paper	N/A
<i>Tnfsf15</i> -gRNA-B1 (TCTGAGTTTGTGTACCTACTGG)	This paper	N/A
<i>Tnfsf15</i> -gRNA-B2 (TTCGTGGCATTCAATGCAACAGG)	This paper	N/A
Primer 7: <i>Tnfsf15</i> -F1 (TGTGTGCTGTGCCCATGTAGAT)	This paper	N/A
Primer 8: <i>Tnfsf15</i> -R1 (CTTTGGAAA CTCACAGAAATCACC)	This paper	N/A
Primer 9: <i>Tnfsf15</i> -F2 (TTGAGGAAACTCAGGCTCAGTC)	This paper	N/A
Software and algorithms		
FlowJo software	Tree star	https://www.flowjo.com/solutions/flowjo/downloads
Prism 6	GraphPad Software	N/A
ImageJ	National Institutes of Health	https://imagej.nih.gov/ij/download.html
Other		
Digital caliper	Mitsutoyo Japan	Cat#PK-1012CPX

RESOURCE AVAILABILITY

Lead contact

Further information and requests for resources and reagents should be directed to and will be fulfilled by the lead contact, Katsuki Sato (katsuki_sato@med.miyazaki-u.ac.jp).

Materials availability

There are restrictions to the availability of the CD103-LSL-DTR mouse lines and B6.*T11a*^{-/-} mouse lines generated in this study due to the need for MTA with University of Miyazaki.

This study did not generate additional new unique reagents.

Data and code availability

- Bacterial 16S rRNA sequencing data reported in this study have been deposited in DNA Data Bank of Japan's BioProject: DRA015912.
- This study does not report original code.
- Any additional information required to reanalyze the data reported in this paper is available from the [lead contact](#) upon request.

EXPERIMENTAL MODEL AND SUBJECT DETAILS

Mice

The following 4- to 12-week-old mice were used in this study: C57BL/6 mice (Japan Clea, Japan), B6N.129S4-Gt(ROSA)26Sor^{tm1(FLP1)Dym/J} mice (FLPeR mice),⁵² and B6.Cg-Tg(*Itgax-cre*)1-1Reiz/J mice³³ (CD11c-Cre mice; The Jackson Laboratory). FLPeR mice and CD11c-Cre mice were cross-mated for more than nine generations with C57BL/6 mice. B6.CD11c:CD103-DTR mice and B6.*T11a*^{-/-} mice were generated as described below. B6.CD45.1⁺OT-I T-cell receptor (TCR) Tg mice harboring OVA-specific CD8⁺ T cells (B6.CD45.1⁺OT-I mice), B6.CD 45.1⁺OT-II TCR Tg mice harboring OVA-specific CD4⁺ T cells (B6.CD45.1⁺OT-II mice), and B6.CD45.1⁺*Foxp3*^{EGFP}OT-II OVA-specific TCR Tg mice harboring OVA-specific CD4⁺*Foxp3*^{EGFP+} T cells (B6.CD45.1⁺*Foxp3*^{EGFP}OT-II mice) were generated as described previously.^{35–37} All mice were bred and maintained under specific pathogen-free conditions in the animal facility at the University of Miyazaki, and all experiments were performed in accordance with institutional guidelines of the Animal Experiment Committee and Gene Recombination Experiment Committee. Female mice were used in all *in vitro* and *in vivo* experiments.

METHOD DETAILS

Generation of CD11c:CD103-DTR mice

B6.*Cd103/Itgae*-LSL-DTR mice, as described for CD103-LSL-DTR mice above, were generated using BAC technology by the insertion of DTR into the *Cd103/Itgae* locus behind a loxP signal-flanked transcriptional STOP cassette by homologous recombination in the 160-kb mouse genomic BAC clone RP23-263M10 (BACPAC Resources). The targeting vector was constructed in the pBluescript vector using a 0.5-kilobase (kb) genomic fragment (left arm) upstream of the stop codon of *Cd103*, and a 0.5-kb genomic fragment (right arm) downstream of the stop codon, which were custom-made using GeneArt® (Life Technologies), and each of the 5'- and 3'-ends was tagged with *Xho*I and *Sal*I sites for the left arm or *Sal*I and *Eco*RV sites for the right arm, respectively. Following the digestion of the 0.5-kb fragment with *Xho*I and *Sal*I, and the 0.5-kb fragment with *Sal*I and *Eco*RV, each fragment was ligated to each site of pBluescript. A *Sal*I restriction site was engineered in place just behind the stop codon in exon 31. The *Loxp-FRT-PGK-gb2-Neo-pA-FRT-Stop-Loxp-IRE2-DTR-EGFP-pA* cassette was cloned into the *Sal*I site inserted into the targeting vector. WT BAC was modified by Red/ET recombination technology (Gene Bridges) as described elsewhere using the targeting vector. The clone insert was released from the vector backbone using *Not*I digestion, gel-purified, and microinjected into the pronuclei of fertilized C57BL/6 oocytes. The founder line with high transgene expression was chosen for further analysis. The mutant mice were genotyped by PCR using Primer 1 (5'- CATTGAAGTATTTAGCATTACAATCCAT-3') and Primer 2 (5'-ATAACCTCCTCCTATGGTACCTAAC-3'). B6.*Cd103/Itgae*-LSL-DTR⁺*Neo*⁺ mice were cross-mated with B6.FLPeR mice to excise the flanked FRT sites by Flp-recombinase to remove the *Neo* cassette, and they were screened by genotyping with PCR using Primer 1 and Primer 2. Heterozygous offspring were crossed to produce homozygous mutant offspring (B6.*Cd103/Itgae*-LSL-DTR⁺; CD103-LSL-DTR mice). CD103-LSL-DTR mice were further cross-mated with B6.CD11c-Cre mice to generate CD11c-Cre:CD103-LSL-DTR mice (CD11c:CD103-DTR mice). CD11c:CD103-DTR mice were genotyped by PCR using Primer 3 (5'-GACCTTTTGAGAGTCACTTTATCCTC-3') and Primer 4 (5'-ATCTTCTGACAACTACGACATGTTCCAC -3'), and Primer 5 (5'-ACTTGGCAGCTGTCTCCAAG-3') and Primer 6 (5'-GCGAA CATCTTCAGTTCTG-3') to detect the CD11c-Cre transgene.³³

Generation of *T11a*^{-/-} mice

B6.*T11a*^{-/-} mice were custom-created using CRISPR/Cas-mediated genome engineering (Cyagen Biosciences, China). The mouse *Tnfrsf15* gene (GenBank accession number: NM_177371.4; Ensembl: ENSMUSG00000050395) is located on mouse chromosome 4. Exon 2 to exon 3 was selected as the target site with deletion of 3.014-kb. Two pairs of gRNA targeting vectors were constructed and confirmed by sequencing. gRNA target sequences were as follows: gRNA-A1 (matching reverse strand of gene): 5'-CAG GCTTGAG-CACGAGACGCAGG-3', gRNA-A2 (matching forward strand of gene): 5'-TACCCTAGACCAGTTAGCACTGG-3', gRNA-B1 (matching reverse strand of gene): 5'-TCTGAGTTTGTGTACCTACTGG-3', and gRNA-B2 (matching forward strand of gene): 5'-TTCGTGGCATTCAATGCAACAGG-3'. The underlining in each sequence indicates PAM (protospacer adjacent motif). Cas9 mRNA and gRNA generated by *in vitro* transcription were co-injected into fertilized eggs for knocked-out (KO) mouse production. The founder line was chosen for further analysis. The mutant mice were genotyped by PCR using Primer 7 (5'-TGTG TGCTGTGCCCATGTAGAT-3') and Primer 8 (5'-CTTTGGAAA CTCACAGAAATCACC-3') with the product of 513 bp for the targeted allele or 3,527 bp for the WT allele, respectively. WT mice were also genotyped by PCR using Primer 8 and Primer 9 (5'-TTGAG GAAACTCAGGCTCAGTC-3') with a product of 721 bp for the WT allele. The KO founders were mated with C57BL/6 mice, and the offspring were screened by genotyping with PCR to establish B6.*T11a*^{-/-} mice.

Cell isolation

Leukocytes were prepared from Spl, PLNs, MesLNs, thymus, SiLP, colonic LP, lung, and bronchoalveolar lavage (BAL), as described previously.^{4,7,14,35-37,49,53} CD11c⁺ DCs were purified by AutoMACS with mouse CD11c (N418) Microbeads (Miltenyi Biotec). Subsequently, CD11c⁺ DCs were sorted into migratory I-A/I-E^{hi}CD11c^{med}CD103⁺CD11b⁻ cDCs, I-A/I-E^{hi}CD11c^{med}CD103⁺CD11b⁺ cDCs, I-A/I-E^{hi}CD11c^{med}CD103⁻CD11b⁺ cDCs, resident I-A/I-E^{med}CD11c^{hi}CD11b⁺ cDCs, and resident I-A/I-E^{med}CD11c^{hi}CD103⁺ cDCs with high purity (each >99%) using a FACSArial cell sorter (BD Biosciences) with fluorescein-conjugated mAbs (BD Biosciences). CD4⁺ T cells were purified from splenocytes of B6.CD45.1⁺OT-II mice (CD45.1⁺Vα2⁺OT-II CD4⁺ T cells), and B6.CD45.1⁺*Foxp3*^{EGFP} OT-II mice (CD45.1⁺*Foxp3*^{EGFP}Vα2⁺CD4⁺ T cells) with mouse CD4 T lymphocyte Enrichment Set-DM and (BD Biosciences). CD8⁺ T cells were purified from splenocytes of B6.CD45.1⁺OT-I mice (CD45.1⁺Vα2⁺OT-I CD8⁺ T cells) with mouse CD8 T lymphocyte Enrichment Set-DM and (BD Biosciences). In some experiments, CD45.1⁺Vα2⁺CD4⁺*Foxp3*^{EGFP-} T cells (CD45.1⁺OT-II CD4⁺*Foxp3*^{EGFP-} T cells) were purified from CD45.1⁺*Foxp3*^{EGFP}Vα2⁺CD4⁺ T cells with >99% purity by a FACSArial cell sorter with fluorescein-conjugated mAbs (BD Biosciences).

BM chimeric mice and DT treatment

BM chimeric mice were generated as described previously.³⁵ In brief, recipient WT mice received 10 Gy of total body irradiation, split into 2 doses separated by 4 hours to minimize gastrointestinal toxicity, and intravenously (i.v.) injected with BM cells (5x10⁶/mouse) from CD11c:CD103-DTR mice. The BM chimeric mice were allowed to rest for 8 weeks before they were used in experiments. For the systemic ablation of CD103⁺ cDCs, CD11c:CD103-DTR → WT chimeras were intraperitoneally (i.p.) injected with DT (1 μg/mouse; Sigma-Aldrich) used as ΔCD11c⁺CD103⁺ cDC mice. In parallel experiments, CD11c:CD103-DTR → WT chimeras were i.p. injected with phosphate-buffered saline (PBS) used as CD103⁺ cDC-sufficient control mice. In another experiment, we generated mixed BM chimeric mice by reconstitution with BM from CD11c:CD103-DTR mice and WT mice or CD11c:CD103-DTR mice and *T11a*^{-/-} mice into lethally irradiated recipient WT mice (CD11c:CD103-DTR/WT → WT mixed chimeras or CD11c:CD103-DTR/*T11a*^{-/-} → WT mixed chimeras, respectively), and they were subsequently i.p. injected with DT or PBS. CD11c:CD103-DTR/*T11a*^{-/-} → WT mixed chimeras that had been treated with DT were used as CD11c⁺CD103⁺*T11a*^{-/-} cDC mice, while CD11c:CD103-DTR/WT → WT mixed chimeras that had been treated with PBS were used as control mice.

Flow cytometry

Cells were stained with fluorescein-conjugated mAbs listed in [key resources table](#). For the intracellular expression of cytokines,⁴ cells were incubated for 4 hrs with phorbol 12-myristate 13-acetate (PMA, 50 ng/mL; Sigma-Aldrich) and ionomycin (IoM, 500 ng/mL; Sigma-Aldrich) plus Brefeldin A (eBiosciences) during the final 2 hrs. Subsequently, the cells were resuspended in Fixation-Permeabilization solution (eBiosciences) and intracellular cytokine staining was carried out according to the manufacturer's directions. To detect ALDH activity,⁴ cells were stained with an ALDEFLUOR staining kit (StemCell Technologies) with or without the ALDH inhibitor diethylaminobenzaldehyde (DEAB, 30 μM; StemCell Technologies) according to the manufacturer's protocol. Fluorescence staining was analyzed with a FACSVerser flow cytometer (BD Biosciences) and FlowJo software (Tree star).

Quantitative reverse transcription polymerase chain reaction (RT-PCR)

Total RNA from cells was extracted using the RNeasy plus micro kit (Qiagen), and the first-strand complementary DNA (cDNA) was synthesized from 100 ng of total RNA with oligo(dT)₂₀ primers using the PrimeScript RT Master Mix (Takara, Japan) according to the manufacturer's instructions. Transcriptional expression levels were analyzed as described previously⁴ using SYBR® Premix Ex Taq II on Thermal Cycler Dice (Takara, Japan) with specific primer pairs listed in [key resources table](#) after normalization for *Gapdh* expression.

In vitro CD4⁺ T cell differentiation assay

For the differentiation of *Foxp3*^{EGFP+} pT_{reg} cells,^{4,7,14} CD45.1⁺OT-II CD4⁺*Foxp3*^{EGFP-} T cells (2×10^4) were cultured with cDCs (5×10^3) in the presence or absence of an active (1 ng/mL; Wako Pure Chemicals, Japan) or a latent (4 ng/mL; R&D Systems) form of TGF- β 1 in combination with OVAp (1 μ M), anti-IFN- γ mAb (10 μ g/mL; R4-6A2, BD Biosciences), and anti-IL-4 mAb (10 μ g/mL; 11B11, BD Biosciences) for 5 days in 96-well round-bottomed plates (BD Biosciences). Analysis of the expression of *Foxp3*^{EGFP} among CD4⁺ T cells was performed by flow cytometry, as described above.

Induction of oral tolerance and immunization with OVA

Mice were intragastrically administered 20 mg of chicken OVA protein (A5503; Sigma-Aldrich) dissolved in PBS.^{4,7} Control mice were given PBS alone. One week after OVA feeding, mice were immunized subcutaneously (s.c.) with 100 μ g of OVA protein emulsified in complete Freund's adjuvant (CFA) (Difco).^{4,7} In some experiments, CD11c:CD103-DTR \rightarrow WT chimeras or CD11c:CD103-DTR/*T11a*^{-/-} \rightarrow WT mixed chimeras were i.p. injected with DT as described above daily for three days before OVA feeding. Two weeks after immunization, sera were obtained from the mice.

Measurement of serum Flt3L

Serum Flt3L was measured using Mouse/Rat Flt-3 Ligand/FLT3L Quantikine enzyme-linked immunosorbent assay (ELISA) kit (R&D Systems).

Measurement of serum OVA-specific Ab

Serum OVA-specific IgG₁ and OVA-specific IgE were assayed using LBIS Mouse OVA-IgG₁ ELISA KIT and LBIS Mouse OVA-IgE ELISA Kit (both from FUJIFILM Wako Shibayagi, Japan), according to the manufacturer's instructions.

DTH

Mice fed with or without OVA protein were s.c. immunized with OVA protein emulsified in CFA, as described above. At 10 days after immunization, the left ear of each mouse was sensitized by i.d. administration with 10 μ g of OVA protein in 10 μ L of PBS, and the right ear was administered an equal amount of PBS as a control using a microsyringe (Lo-dose insulin syringe 0.3 cc with 30 G; Becton-Dickinson). OVA-specific DTH was determined by the ear thickness at various days after sensitization for 4 days using digital calipers (PK-1012CPX; Mitsutoyo, Japan).⁴ Alternatively, ear or sera were obtained from the mice at 2 or 7 days after sensitization.

Airway inflammation in response to OVA

On days 7 and 14 after OVA feeding, mice were i.p. immunized with 100 μ g of OVA protein emulsified in alum (4 mg; Imject Alum; Thermo Scientific). Subsequently, mice were i.n. challenged with 200 μ g of OVA protein in 40 μ L of PBS or PBS alone as a control on days 14, 15, and 16 after the last immunization. At 17 days after the last immunization, sera, BALF, and lung samples were obtained from the mice.^{4,14}

Adoptive transfer

For Ag-specific priming of CD4⁺ T cells or CD8⁺ T cells *in vivo*,^{14,35–37} CD45.1⁺OT-II CD4⁺ T cells or CD45.1⁺OT-I CD8⁺ T cells were labeled with Cell Proliferation Dye eFluorTM 670 (eBioscience; 5 μ M) at 37°C for 10 min, and washed twice with cold PBS. Subsequently, eFluorTM 670-labeled CD45.1⁺OT-II CD4⁺ T cells or CD45.1⁺OT-I CD8⁺ T cells (each 5×10^6 /mouse) were i.v. injected into mice 24 hrs before oral administration of OVA protein. After two days, the gated CD45.1⁺OT-II CD4⁺ T cells or CD45.1⁺OT-I CD8⁺ T cells in MesLNs were analyzed for eFluorTM 670 dilution to detect the dividing cells by flow cytometry. For the differentiation of *Foxp3*^{EGFP+} pT_{reg} cells *in vivo*,^{14,35,36} mice were i.v. injected with CD45.1⁺OT-II CD4⁺*Foxp3*^{EGFP-} T cells (2×10^6 /mouse), and then orally administered 50 mg of OVA protein on days 0 and 1. On day 2, the expression of *Foxp3*^{EGFP} among gated CD45.1⁺OT-II CD4⁺ T cells was analyzed by flow cytometry.

Histopathologic assessment

Tissues from the ear and lung were fixed with 4% paraformaldehyde (PFA) in PBS and embedded in paraffin. The tissue sections (5- μ m thickness) were stained with H&E and PAS,^{4,14} The stained slides were examined with bright-field microscopy (BX53; Olympus, Japan). The areas of the epidermis and dermis of the ear were quantified by thickness using ImageJ (National Institutes of Health) by a blinded observer, as described previously.⁴

Immunohistochemical analysis

MesLNs were embedded in OCT compound (Sakura Finetek, Japan) and frozen in liquid N₂. Each frozen section (7 μ m) was fixed with cold acetone, and blocked with PBS containing 5% normal rat serum. Subsequently, the slide was stained with Alexa Fluor 488-conjugated anti-CD11c mAb, PE-eFluor 610-conjugated anti-CD19 mAb, and Alexa Fluor 647-conjugated anti-CD103 mAb, and mounted with SlowFade Diamond Antifade Mountant (Invitrogen). Alternatively, the slide was stained with Alexa Fluor 594-conjugated anti-CD11c mAb, APC-conjugated anti-CD3 ϵ mAb, and Alexa Fluor 488-conjugated anti-CD45R/B220 mAb, and mounted with SlowFade Diamond Antifade Mountant. In another experiment, paraffin-embedded MesLNs were cut into sections

(4 μm) and placed onto silane-coated slide glasses. The sections were deparaffinized with toluene and rehydrated using a graded ethanol series, then autoclaved at 120°C for 15 min in 10 mM citrate buffer (pH 6.0). After inhibition of endogenous peroxidase activity with 3% H_2O_2 in methanol for 30 min, the sections were pre-incubated with 500 $\mu\text{g}/\text{mL}$ normal goat IgG (Sigma) and 1% BSA in PBS for 1 h to block non-specific binding of Abs. The sections were then reacted with the following primary antibodies overnight: anti-CD3 mAb (Abcam), Alexa Fluor 488-conjugated anti-Foxp3 mAb (Biolegend) and anti-ROR γ mAb (eBiosciences). After washing with 0.075% Brij L23 (Sigma) in PBS, the sections were reacted with HRP-goat anti-rat IgG (Millipore) or HRP-goat anti-rabbit IgG (Dako) for 1 h. After washing in 0.075% Brij L23 in PBS, the HRP-sites were visualized with FITC-conjugated tyramide (Invitrogen). Then, the next primary antibody was reacted overnight, and its detection was repeated with rhodamine conjugated tyramide (Invitrogen) and then counterstained with DAPI (Invitrogen). The stained slides were analyzed with a BZ-X710 fluorescence microscope (KEYENCE, Japan).

Antibiotic treatment

Depletion of commensal bacteria was performed using antibiotics according to previous reports^{19,22} with some modifications. In brief, 4-week-old mice were given sterile distilled water with or without kanamycin (0.5 mg/mL; Wako Pure Chemicals, Japan), gentamicin (0.35mg/mL; Wako Pure Chemicals, Japan), metronidazole (1 mg/mL; Wako Pure Chemicals, Japan), colistin (0.5 mg/mL; Wako Pure Chemicals, Japan), and vancomycin (0.225 mg/mL; Wako Pure Chemicals, Japan) continuously via a water bottle for four weeks. PBS was used as a control.

Tumor transplantation for overexpression of *Csf2*

The B16-F10 murine melanoma cell line (B16), kindly provided by Dr. Shin-ichiro Fujii (RIKEN Center for Integrative Medical Sciences, Japan), and *Csf2*-transfected derivative of B16-F10 cells (B16^{*Csf2*})⁴⁶ (RIKEN BioResource Center, Japan) were cultured in DMEM (Wako Pure Chemicals, Japan) supplemented with 10% heat-inactivated fetal calf serum (FCS; Gibco) at 37°C in a humidified atmosphere of 5% CO_2 and air. Mice that had received oral combinatorial antibiotic treatment for four weeks, as described above, were inoculated s.c. with B16 or B16^{*Csf2*} (1×10^5) into the back skin, and then subjected to continuous oral combinatorial antibiotic treatment. Animals were monitored daily and analyzed 10-15 days after inoculation.

Agonistic anti-DR3 mAb administration

Mice were i.p. injected with 2.5 μg of agonistic anti-DR3 mAb (4C12; Biolegend)⁴⁵ 2 days before OVA feeding, as described above. Control mice were injected with PBS alone. In some experiments, MesLNs were obtained from the mice on the next day or 2 days after injection.

16S rDNA sample acquisition, quantification, and analysis of 16S rDNA

16S rRNA metagenomic analysis was performed at Repertoire Genesis (Japan). In brief, microbial DNA was extracted from frozen murine fecal samples of SI using Isospin fecal DNA (NIPPON GENE, Japan). For bioinformatics analysis of 16SrRNA, the V3V4 region of 16S rRNA genes was amplified and sequenced by MiSeq Deep sequencer and MiSeq Reagent Kit v3 (Illumina) following the manufacturer's instructions. The sequence data were preprocessed and analyzed using the Flora Genesis software (Repertoire Genesis, Japan). In brief, the R1 and R2 read pairs were joined and chimera sequences were removed. Operational taxonomic unit (OTU) picking was performed by the open-reference method using the 97% ID prefiltered Greengenes database and uclust. Representative sequences of each OTU were chosen and taxonomy assignment was performed by the ribosomal database project (RDP) classifier using a threshold score of 0.5 or more. The OTUs were grouped if their annotation was the same regardless of the RDP score.

QUANTIFICATION AND STATISTICAL ANALYSIS

All statistical analysis was performed using Prism 6 (GraphPad Software). Data are expressed as the mean \pm s.d from three to thirteen individual samples in a single experiment, and we performed at least three independent experiments. The significance of the differences between the values obtained was evaluated by unpaired two-tailed Student's t test. A P value of < .05 was considered significant.